MASTER THESIS

The effect of hip and knee joint calibration methods on muscle-tendon length and velocity in modelling gait

By E.B. Pietersma

TU Delft Delft University of Technology

THE EFFECT OF HIP AND KNEE JOINT CALIBRATION METHODS ON MUSCLE-TENDON LENGTH AND VELOCITY IN MODELLING GAIT

MASTER THESIS

By E.B. Pietersma

For the degree Master of Science in Biomedical Engineering
at Delft University of Technology

Supervisors:
Prof. dr. H.E.J. Veeger
Dr. M.M. van der Krogt
Prof. dr. T. Geijtenbeek

11th of July, 2014

ABSTRACT

Musculoskeletal modelling can be used to predict the need and effectiveness of muscle-tendon (MT) lengthening in Cerebral Palsy (CP) patients by evaluating MT length and velocity during gait. MT length and velocity are strongly related to the position and orientation of the joints. In clinical gait analysis, hip and knee joint coordinate systems can be determined based on anatomical markers combined with regression equations or using different functional calibration methods.

The goal of this study is to investigate to what extend marker-based versus functional calibration methods affect hip and knee coordinate systems, how this influences muscle-tendon length and velocity when modelling gait and what the possible effect on clinical decision-making might be.

Three healthy adult subjects (1 male, 1.95 m, 96 kg, 2 female, 1.68 and 1.66 m, 65 and 69 kg, all between 20 and 25 years) underwent gait analysis on an instrumented treadmill, while performing unimpaired and CP mimicking gait. Marker-based (MB) joint calibration was done with the use of anatomical landmarks combined with regression equations, and functional calibration (FC) with the use of a least square sphere fit method for the hip and mean instantaneous helical axis for the knee. The effect of joint calibration on MT lengths and velocities of four typical lower extremity muscles were compared between MB and FC models. Furthermore, the effect of adding a sliding knee, rather than a fixed hinge knee joint, was evaluated. MT modelling output of the CP gait trials was evaluated with similar criteria as used in clinic to give an indication of the possible effect of the use of different joint calibration methods on clinical decision-making.

Functional calibration altered the hip joint centre location by 51.0 ± 19.5 mm, the knee centre location by 38.7 ± 21.7 mm and the knee axis orientation by 14.3 ± 8.2°, compared to the MB joint coordinate systems. The overall effect of joint calibration methods on MT length and velocity is small, but is most visible in MT lengths and to a lesser extend in MT velocities. Mean differences in peak MT length varied up to 17.1% as a percentage of the peak MT length of the MB model. Mean peak MT velocity differences ranged up to 9.85% as a percentage of the range of velocity. Knee translation had a negligible effect on MT lengths, but did affect MT velocity with mean peak differences up to 16.85%. 4 out of 24 clinical decisions were altered as a result of functional calibration and 6 out of 24 as a result of knee translation.

Joint calibration methods have a large effect on joint coordinate systems in healthy subjects, with a presumably even more present effect in CP patients with severe bone deformities. Although the effect of calibration methods on MT length and velocity is small, this might still influence clinical decision-making. This clinical relevance denotes the need for further research in investigating suitable calibration methods for gait analysis of CP patients.

Keywords: calibration - joint - musculoskeletal - modelling - gait - Cerebral Palsy - muscle-tendon

TABLE OF CONTENT

PREFACE ..... **VI**
ACKNOWLEDGEMENTS ..... **VII**
1 INTRODUCTION **1**
1.1 Background **1**
1.2 Problem statement **1**

2 METHODS **3**
2.1 Subjects **3**
2.2 Experimental setup **3**
2.3 Calibration methods **4**
2.3.1 Marker-based calibration 4
2.3.2 Functional calibration 4
2.4 Models **6**
2.4.1 Marker-based and functional models 6
2.4.2 Sliding knee models 7
2.5 Data analyses **8**

3 RESULTS **10**
3.1 Joint calibration **10**
3.1.1 Hip joint calibration 10
3.1.2 Knee joint calibration 11
3.1.3 Segment lengths 12
3.2 MT length and velocity **12**
3.2.1 Effect of calibration methods 12
3.2.2 Effect of knee translation 13
3.2.3 UI versus CP gait data 13
3.2.4 Effect on clinical decision-making 17

4 DISCUSSION **19**
5 CONCLUSION **21**
6 GLOSSARY **22**
7 REFERENCES **23**
8 APPENDICES **25**
Appendix A Equipment **25**
Appendix A.1 Straps for mimicking CP gait 25
Appendix A.2 GRAIL 26
Appendix B Lower extremity marker set **27**
Appendix C Joint calibration **29**
Appendix C.1 Hip joint calibration 29
Appendix C2 Knee joint calibration 32
Appendix D | Kinematics **37**
Appendix D.1 Conclusions and remarks 37

Appendix E Kinetics **40**
Appendix E1 Joint moments 40
Appendix E2 Conclusions and remarks 40
Appendix E3 Joint power 43
Appendix E4 Conclusions and remarks 43
8.2 Appendix F | Muscle-tendon outcome **46**
Appendix F1 | Muscle-tendon length 46
8.2.1 Appendix F2 | Muscle-tendon velocity 50

List of Figures

Figure 1. Motion trails for functional calibration 3
Figure 2. Functional joint calibration 5
Figure 3. Functional models 6
Figure 4. Knee translation curves 8
Figure 5. Flow chart for collecting and analysing data 8
Figure 6. MT length and velocity MB and FC models 15
Figure 7. MT length and velocity KF and SK models 16
Figure 8. Effect on clinical decision-making 17
Figure 9. Straps to restrict knee flexion 25
Figure 10. GRAIL 26
Figure 11. Experimental and virtual marker set 27
Figure 12. Pelvis coordinate system 29
Figure 13. Marker-based hip joint calibration 30
Figure 14. Functional hip joint calibration 31
Figure 15. Marker-based knee joint calibration 32
Figure 16. Femur and tibia coordinate systems 32
Figure 17. IHA of loaded and unloaded knee 34
Figure 18. IHA loaded knee 34
Figure 19. IHA unloaded knee 35
Figure 20. Joint angles of average subject 38
Figure 21. Joint moments of average subject 41
Figure 22. Joint power of average subject 44
Figure 23. MT lengths of average subject absolute and normalized 47
Figure 24. MT velocities of average subject absolute and normalized 51

LIST OF TABLES

Figure 1. Motion trails for functional calibration 3
Figure 2. Functional joint calibration 5
Figure 3. Functional models 6
Figure 4. Knee translation curves 8
Figure 5. Flow chart for collecting and analysing data 8
Figure 6. MT length and velocity MB and FC models 15
Figure 7. MT length and velocity KF and SK models 16
Figure 8. Effect on clinical decision-making 17
Figure 9. Straps to restrict knee flexion 25
Figure 10. GRAIL 26
Figure 11. Experimental and virtual marker set 27
Figure 12. Pelvis coordinate system 29
Figure 13. Marker-based hip joint calibration 30
Figure 14. Functional hip joint calibration 31
Figure 15. Marker-based knee joint calibration 32
Figure 16. Femur and tibia coordinate systems 32
Figure 17. IHA of loaded and unloaded knee 34
Figure 18. IHA loaded knee 34
Figure 19. IHA unloaded knee 35
Figure 20. Joint angles of average subject 38
Figure 21. Joint moments of average subject 41
Figure 22. Joint power of average subject 44
Figure 23. MT lengths of average subject absolute and normalized 47
Figure 24. MT velocities of average subject absolute and normalized 51

PREFACE

This thesis describes the main work that I have done during my final project as part of the MSc program in Biomedical Engineering at the Delft University of Technology. The report aims on providing better insight in the clinical relevance of joint calibration methods in musculoskeletal modelling of healthy subjects or subjects with a certain pathology such as Cerebral Palsy.

The scope of this thesis originates from the objectives of the paediatric biomedical project MD-Paedigree, which is a clinically-driven and strongly Virtual-Physiologic-Human-rooted project in cooperation with world-renowned clinical centres and other partners including the Delft University of Technology, Motek Medical B.V. and the medical centre of the VU medical centre Amsterdam. The latter parties were all involved in this project.

A part of my project I have fulfilled during my internship at Motek Medical B.V. This has been a great introduction to working in the Biomedical field. I have learned that working in a multidisciplinary team is not only very educational, but can also be of great value for innovative and creative product solutions.

During my project I enjoyed the experiments that I carried out. Looking back, I would have done a lot of things differently, but of course this makes it a good learning experience. Overall, I think this final project showed me that I am able to individually apply the knowledge that I have gained during my studies, which gives me confidence to make the next step into the 'professional world'.

ACKNOWLEDGEMENTS

First, I would like to express my very great appreciation to my graduation committee: Dirkjan Veeger for his supervision and guidance during the project, Marjolein van der Krogt for her useful critiques and willingness to help through all times and Thomas Geijtenbeek for the inspiration and review of my work.

Secondly, I would like to thank Frans Steenbrink and Ben van Basten for giving me the opportunity to fulfil part of my thesis project at Motek Medical and the rest of the employees for letting me observe their daily operations. The possibility to use the motion capture equipment of Motek Medical when needed was greatly appreciated and I would especially like to thank Sanne Roeles and Edwin van Loon for their help during my experiments. Also all volunteers to my experiments are acknowledged.

Finally, I could not have completed my study without the support of my family and friends.

Elisah Pietersma
11th of July 2014

1 INTRODUCTION

1.1 Background

Cerebral Palsy (CP) is a motor disorder caused by brain damage at early childhood. The prevalence of CP ranges from 2 to 2.5 per 1000 live births in the western world [1]. CP is characterised by tight muscles, causing movement abnormalities. Muscles are considered tight when they operate at abnormally short muscle-tendon (MT) length or show a velocity-dependent resistance to stretch resulting in abnormally low MT velocities. The most common gait abnormality among CP patients is crouch gait, which is characterised by excessive flexion of the knee and hip during stance that is often a result of short or slow hamstrings and hip flexor muscles [2]. Equinus gait is another frequently occurring gait abnormality of which excessive plantar-flexion of the ankle due to tight calf muscles is thought to be a possible cause. A common treatment for the restricted movement as a result of tight muscles is surgical muscle or tendon lengthening [3, 4]. Many clinical studies have been conducted in order to investigate the effectiveness of tendon lengthening, resulting in unpredictable and often inconsistent results. DeLuca, et al. [5] showed that the success of tendon lengthening largely depends on the treatment of the correct muscle or combination of muscles. The research of Arnold, et al. [6] on the other hand showed that tendon lengthening is only effective when a patient's muscles operate at lengths and velocities that are too short or too low.

Musculoskeletal (MS) modelling can be a helpful tool in analysing muscle behaviour during gait and can therefore be used to predict the need and effectiveness of MT lengthening. By comparing peak MT length and velocity of CP patients with average unimpaired gait data too short or too slow muscles can be distinguished [6, 7].

1.2 Problem statement

MT geometry needs to be modelled accurately in order to predict whether CP patients would benefit from MT lengthening. MT length and velocity are strongly related to the joint and segment kinematics, which indicates that a patient's joint locations and orientations need to be closely matched for accurate MT length and velocity estimation. Delp, et al. [2] and Arnold, et al. [6] have already studied the usage of a generic MS model in estimating MT lengths. In this generic model however, the location and orientation of the joints are based on healthy MS morphology and might therefore not represent MS abnormalities that are prevalent in CP patients, such as bone deformities. Arnold, et al. [8] studied the effect of bone deformities by comparing MT lenghts estimated by a generic model, with estimations based on a personalised deformable femur. With the use of MR imaging techniques the femoral anteversian angle, the neck shaft angle and the lesser trochanter torsion angle were adjusted to closely match the femur geometry of the subjects. A maximum difference of 1 standard deviation (SD) in peak length was found, suggesting that personalised segment geometry is needed for accurate MT estimation. Due to costs and invasiveness however, a personalised MR-based model is not applicable for a typical gait analysis lab.

Less invasivaly, the geometry of MS model segments can also be personalised with the use of various scaling techniques. Conventional scaling methods make use of the positions of

palpatable anatomical landmarks (AL). The locations of these landmarks can either be used to esimate joint centers with regression equations that are based on anthropometric measurements [9, 10], or to functionally determine coordinate systems by using the kinematic position of the ALs while moving the joints through their range of motion. It has been shown that functional calibration methods provide more accurate hip joint center estimations in healthy subjects than marker-based regression methods [11].
It can be assumed that this effect will be more present when calibrating joints in CP patiens due to severe bone deformities. However it is unclear what the effect of these different calibration methods is on MS model outcome such as MT length and velocity. When differences in joint calibration methods lead to significantly different model outcome, this might affect clinical decision-making.
The aim of this study was to investigate the effect of marker-based and functional hip and knee joint calibration methods on MT length and velocity in modelling unimpaired and CP gait. The behaviour of four typically tight muscles were studied during gait in order to investigate the effect of different calibration methods and to what extend this might influence clinical decission-making. This insight can either be used to better support clinical decision-making or to improve current models with a more advanced calibration method if the effect on the output is shown to be substantial. Related to this the following research question can be formulated:

What is the effect of marker-based and functional hip and knee calibration methods in terms of estimated muscle-tendon length and velocity when modelling gait?

2 METHODS

2.1 Subjects

Three healthy adult subjects (1 male, 1.95 m, 96 kg, 2 female, 1.68 and 1.66 m, 65 and 69 kg, all between 20 and 25 years) volunteered in this study. Subjects will be further referred to as subject 1, 2 and 3, respectively.

2.2 Experimental setup

Gait data of each subject was obtained by instructing the subjects to perform unimpaired (UI) gait and mimicked CP gait on an instrumented treadmill. The subjects were allowed to become familiar with walking on the treadmill for a few minutes before starting data collection. UI gait data was collected at a speed of 1 m/s and CP gait at 0.65 m/s. The subject received no instructions for the UI gait trial. To mimic CP gait, subjects were equipped with a band attached to the waist and ankles to restrict knee extension (Appendix A1| Straps for mimicking CP gait). This also forced the subjects to walk on their forefeet. The subjects were instructed to perform internal rotation of the foot, but no actions were taken to ensure that this pose was maintained throughout the trial.
The data needed for joint calibration was obtained in two ways: one static trial where the subject was instructed to stand in anatomical position [12] and one functional trial where the subjects were asked to move their lower extremity joints through the range of motion (Figure 1). The data for functional hip calibration was obtained by instructing the subjects to perform a series of hip ante- and retro-flexion, ab- and adduction and a combination of both. Maximum flexion and abduction angles of 40° were achieved. The data for knee calibration was obtained by a series of squat movements, and a series of unloaded knee flexion for each leg. Knee flexion angles ranged from approximately 0° to 80°. All motion trials for functional calibration were repeated three times for each subject.

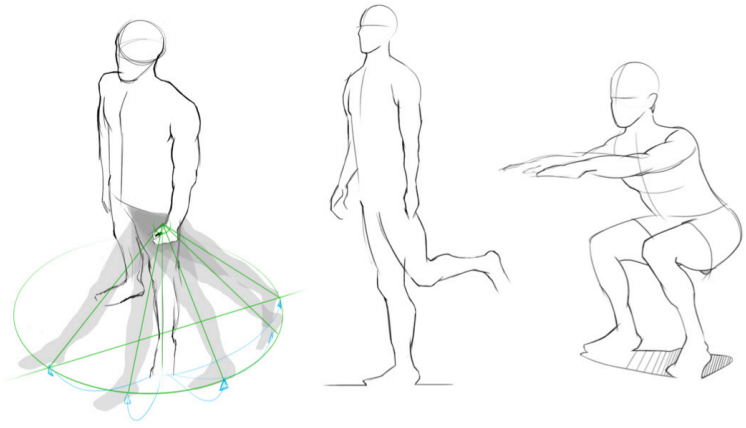

***Figure 1**. Motion trails for functional calibration*
Obtaining functional motion data by moving limbs trough their range of motion. Left: hip flexion/extension and ab/adduction. Middle: unloaded knee flexion. Right: loaded knee flexion.

The motion data was recorded with the GRAIL motion capture system (Appendix A2 | GRAIL) supported by Vicon Giganet hardware, including 8 motion capture cameras, 2 video cameras, an instrumented dual belt treadmill with integrated force plates to measure ground reaction forces and 29 experimental markers. Experimental markers were placed on the ALs of the subject similar to the Motek Human Body Model lower extremity marker set [13] extended with 4 additional markers that were placed on the medial epicondyles and malleoli of the knee and ankle (Appendix B | Lower extremity marker set).

2.3 Calibration methods

The hip and knee joint coordinate systems were calibrated in two ways using either the static trail or the functional trail. All recorded marker data needed for calibration was filtered with a second order Butterworth filter with a cutoff frequency of 6 Herz to reduce skin movement artifacts and other noise before further calculations were made.

2.3.1 Marker-based calibration

Marker-based (MB) calibration was done using only the static marker data. The joint coordinate systems were calibrated with the use of regression equations based on anthropometric measurments. The hip joint centers were estimated with the algorithm proposed by Bell, et al. [9], (Appendix C1.1 | Marker-based hip joint calibration). The knee joint center was defined as the midpoint of the axis through the medial and lateral eypcondyles, this transepicondylar axis was also chosen to be the knee axis of rotation (Appendix C2.1 | Marker-based knee joint calibration).

2.3.2 Functional calibration

Functional calibration (FC) was done with the use of the functional motion trials. Figure 2 shows the methods for calibrating hip and knee joints with the use of the functional marker data.

The hip joint centre was defined as the pivot point of the femur relative to the pelvis, which was determined with the use of a least square sphere fit method, similar to the method proposed by Leardini, et al. [11],(Appendix C1.2 | Functional hip joint calibration). The location and orientation of the knee axis of rotation was determined with the use of the instantaneous helical axis (IHA) method presented by Woltring [14], (Appendix C2.2 | Functional knee joint calibration). The IHA is the line about and along which one segment is instantaneously moving in respect to the other segment. Because the IHA is a kinematic entity it can only be defined during movement. Furthermore, the angular speed must also be sufficiently large to reduce the effect of noise. For this reason only angular velocity larger than 10% of the maximum velocity was used to calculate the IHA. Assuming that the knee can be modelled as a hinge, the axis of rotation can be computed as the mean of a set of instantaneous helixal axes. The knee joint centre was taken to be the point on the mean IHA intersecting the miplane between the epicondyles. The IHA was calculated during both loaded and unloaded knee flexion. The direction and location of the IHA of the loaded knee appeared to be dependant on the flexion angle (Appendix D | figure 18. IHA loaded knee). This was in accordance to the findings of Blankevoort, et al. [15] and implies that small translations occur in the knee joint. The IHA calculated with unloaded knee flexion was

found to be more constant and showed less correlation with the knee flexion angle. Because the loaded stance phase in gait covers the main part of the gait cycle it was decided to calculate the mean IHA with the use of the loaded knee motion data. Corresponding to the range of knee flexion during the stance phase in healthy gait, only the motion data associated with flexion angles between 0° and 40° were selected. Because the IHA of the loaded knee showed clear translations, it was decided to also study the differences between a perfect hinge and sliding knee.

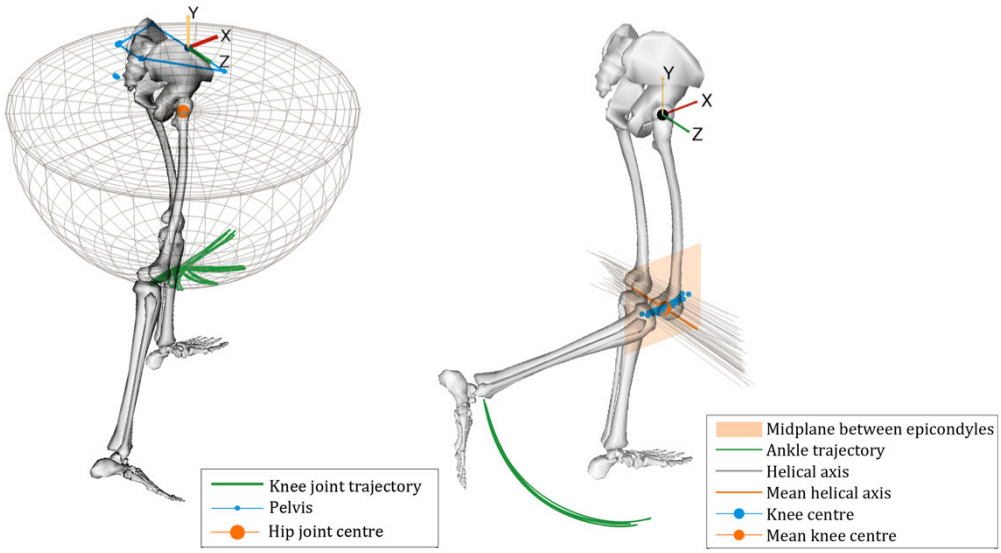

***Figure 2**. Functional joint calibration*
Left: hip joint calibration with the use of a least square sphere fit. Right: knee joint calibration by calculating mean helical axis. Here the IHA determination of the unloaded knee is shown.

In conclusion hip and knee joint coordinate systems were obtained for each leg of all subjects using both MB and FC methods. Hip joint centres were presented in the local coordinate system of the pelvis as can be seen in Appendix D | (Figure 12. Pelvis and knee joint centres, axis orientations and translations are presented in the local coordinate system of the femur as shown in Appendix D | (Figure 16. Femur and tibia coordinate systems).

2.4 Models

The generic Gait2392 model [16] was scaled with the use of OpenSim modelling software [17]. Scaling was done on segmental level with MB anatomical landmarks or with FC joint centres. By matching the location of at least two predefined points per segment on the subject with the same points on the unscaled model, a scaling factor per segment was calculated. This scaling factor was used to scale each segment of the model. All other model parameters such as mass, MT lengths and optimal muscle fibre length are scaled accordingly. OpenSim does not alter the orientation of the coordinate systems of the individual segments during scaling. After scaling the model the virtual markers that were not used for scaling are placed on the model by matching the locations of the experimental marker locations in a static pose.

2.4.1 Marker-based and functional models

In order to examine the effect of both hip and knee joint calibration independently four models were composed (Figure 3). For the first MB model the generic model was scaled with the use of the marker data obtained in the static trials only. Joint coordinate systems were based on regression equations as described in the previous section. In the second model (HF) the hip joint centres were scaled according to the functional hip calibration method. For the other scaling points the AL positions were used. The third model (KF) was scaled with the functionally calibrated knee joint centre. After scaling the direction of the knee axis of rotation in the model was altered in correspondence with the direction of the mean IHA. The fourth model (HKF) was scaled using both the functionally calibrated hip and knee centre location and orientation.

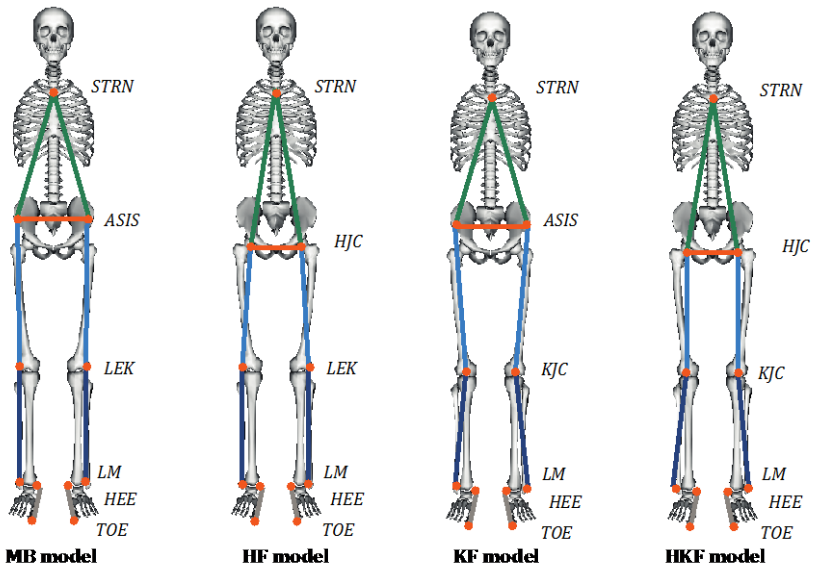

Figure 3. *Functional models*
Models scaled with different scaling points. From left to right: marker-based (MB) model, functional hip (HF) model, functional knee (KF) model and functional hip and knee (HKF) model. STRN: sternum marker, ASIS: right/left anterior superior iliac spline marker, LEK: lateral epicondyle marker, LM: lateral malleolus marker, HEE: heel marker, TOE: toe marker, HJC: hip joint centre, KJC: knee joint centre.

2.4.1.1 Segment lengths

As a result of the different locations of the joints centres, segments lengths are also altered. Pelvis width is measured from hip to hip centre, femur length from hip to knee centre and tibia length from knee to ankle joint centre. Table 1 shows whether the segment lengths of the different models are determined by MB or FC joint locations.

Table 1. *Composition of segment lengths.*
Segmental composition of the different models with segment lengths that are either based on MB or FC joint centres.

Models	Pelvis	Femur	Tibia
MB	MB	MB	MB
HF	FC	MB	MB
KF	MB	FC	FC
HKF	FC	FC	FC

2.4.2 Sliding knee models

The knee joints of the previously described models are modelled as a pure hinge. However small translations were demonstrated during the IHA calculations of the loaded knee flexion as was described in the previous section 2.3.2. To investigate the effect of modelling the knee as a sliding hinge, rather than a perfect hinge, additional sliding knee (SK) models were constructed. This was done by adding flexion angle dependant knee translations to the knee joints of the existing KF models. Due to the limited number of subjects it was not possible to determine a reliable knee translation curve associated with gait from the available data in this study. For this reason it was decided to use the knee translation curves as proposed by *Delp*, Loan et al. (1990), (Figure 4 | grey line) for the first sliding knee model (KF-D). The translation curves of Delp are based on loaded knee flexion ranging from 0° to 100° and describe translations along the sagittal and longitudinal axis over the complete range of knee flexion. This implies that the model also demonstrates knee translation during the unloaded swing phase in every gait cycle, however according to the calculations of the IHA in unloaded condition the knee behaves more like a pure hinge (Appendix D | Figure 17. IHA of loaded and unloaded knee). Therefore a second knee translation model (KF-S) was made where only a translation in the *stance* phase was prescribed. Translation curves for this model are also based on the curves of Delp, but were levelled off after 40 degrees of knee flexion, which on average represents the knee angle during toe off [18], (Figure 4 | green line).

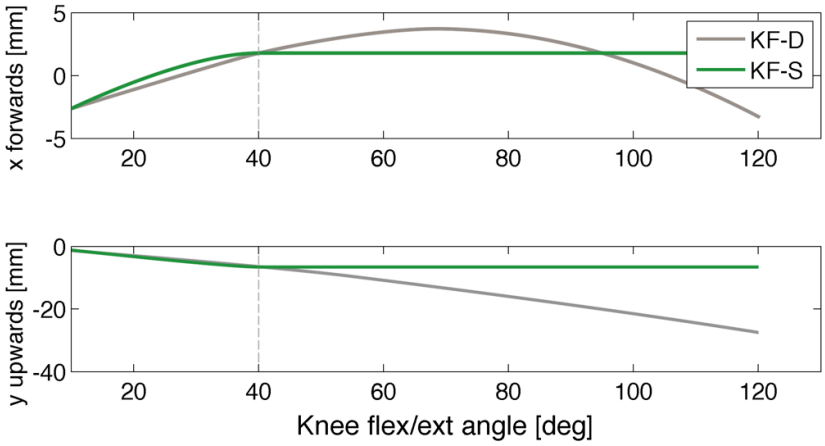

Figure 4. *Knee translation curves*
Knee translation curves as proposed by Delp (grey line) and translation only occurring during stance phase and remains constant after 40° of knee flexion (green line).

2.5 Data analyses

In total six different models were used to simulate the UI and CP gait of each subject: one MB model, three FC models and two SK models. Figure 5 shows the process of the data collection and analysis.

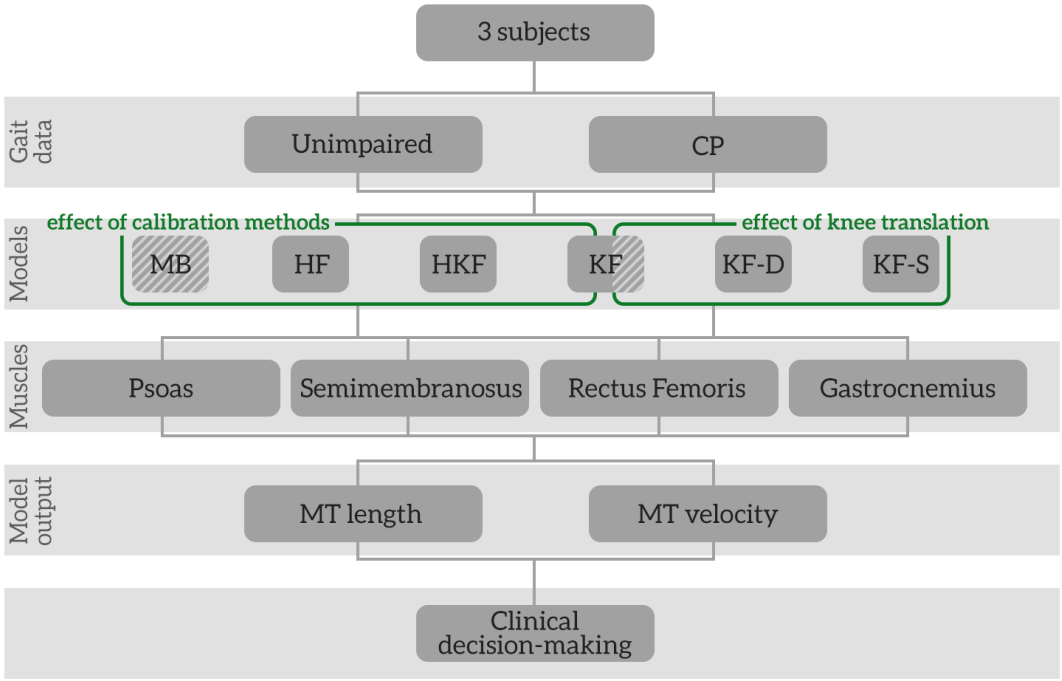

Figure 5. *Flow chart for collecting and analysing data*

To simulate the gait patterns of each subject, the recorded marker trajectories of the UI and CP gait trials were fed to the six different models. The model outcome of the MB the models was used as a reference to evaluate the effect of functional hip and knee calibration. The SK model outcomes were compared to the KF model to evaluate the effect of knee translation.
Four typically tight muscles that are often subjected to surgery in attempt to improve stiff gait in CP patients were evaluated. The psoas muscle that is crossing the hip joint, the semimembranosus and the rectus femoris muscles, crossing both the knee and hip joint and the gastrocnemius muscle, crossing the knee and ankle joint.
MT lengths of the selected muscles were retrieved from the software and MT velocity was estimated by computing the numerical derivative of MT length with respect to time. All data was averaged over at least three gait cycles to reduce irregularities. MT lengths and velocities of the different models were evaluated on peak data, because the peak values are most indicative in clinic. Differences in peak MT length of the FC and SK models compared to the MB or KF models were presented as a percentage of the peak MT length of the MB or KF model. Differences in peak MT velocity were presented as a percentage of the range of velocity of the MB or KF model. Given the small number of subjects, results were evaluated for each subject individually. Also the average peak MT differences of each model were presented.
In order to examine the effect of calibration methods on clinical decision-making, the MT output associated with the CP gait data was evaluated with criteria similar to those used in clinically to distinguish too short or too slow muscles. When this decision based on FC and SK models differs from MB model based findings, this could influence clinical decision-making. A muscle is considered too short or too slow if peak MT length or velocity is lower than the average unimpaired data plus two times the SD [7]. To account for differences in size, MT lengths and velocities are normalised with MT rest length as was also done in the research of Delp, et al. [2] and Thompson, et al. [19]. Because a population of three subjects was too small to calculate a meaningful S.D., the S.D. as was presented by Arnold, et al. [7] for the semimembranosus muscle length and velocity was taken. It was assumed that the SDs for the remaining three muscles are comparable, therefore the same SD as a percentage of MT length was used.

3 RESULTS

3.1 Joint calibration

Joint calibration methods led to different hip and knee joint centres for the hip joint and different knee axis orientations. Functional calibration of the knee also showed a translation of the knee in stance phase. The results for the hip and knee joint calibration are presented in the following sections. Also the effect of the MB and FC joint locations on segment length is shown.

3.1.1 Hip joint calibration

Table 2 shows the location of hip joint centres as a result of MB and functional calibration for each subject. Data needed for calibration of the left hip of subject 3 did not appear to be useful due to too small hip flexion angles. For further use the relative location of the right hip expressed in the pelvis coordinate system was mirrored to the left hip for this particular subject.

Table 2. *Hip joint calibration*
Marker based (MB) and functionally calibrated (FC) hip joint centre locations for the left and right hip of each subject.

		Left hip			**Right hip**		
		x	*y*	*z*	*x*	*y*	*z* [a]
Subject 1	MB (mm)	-66.02	-86.85	104.22	-70.95	-86.75	-104.09
	FC (mm)	-94.63	-100.54	101.51	-99.93	-87.10	-87.30
	Difference (mm) [b]	*31.83*			*33.49*		
Subject 2	MB (mm)	-116.49	-77.95	93.54	-93.71	-77.95	-93.54
	FC (mm)	-64.09	-132.09	86.61	-65.88	-137.43	-86.73
	Difference (mm)	*75.66*			*66.02*		
Subject 3	MB (mm)	-104.93	-80.05	96.06	-105.11	-79.73	-95.68
	FC (mm)	-77.70	-119.57	98.88	-	-	-
	Difference (mm)	*48.06*			-		
		x		*y*		*z*	
Mean[c]	MB (mm)	-92.86 ± 20.27		-81.55 ± 4.16		97.86 ± 4.99	
	FC (mm)	-80.47 ± 16.34		-115.35 ± 21.23		92.21 ± 7.36	
	Difference (mm)	*51.01 ± 19.47*					

[a] *Locations presented in pelvis coordinate system: x-axis pointing forward, y-axis pointing upward, z-axis pointing to the right.*
[b] *Global distance between MB and FC hip joint location.*
[c] *For the mean location in z-direction absolute values are used.*

3.1.2 Knee joint calibration

Table 3 shows the results of the MB and FC knee joint calibration for all subjects. Also the mean values are presented. The joint centre locations are expressed in the local reference frame of the femur. The distance between the MB and FC joint centres and the orientation of the FC knee axis of rotation relative to the MB axis are given as well as the knee translations. An extensive overview including calibration data associated with the unloaded knee motion data can be found in Appendix C2 | Knee joint calibration.

Table 3. *Knee joint calibration*
Marker based and functional knee joint centre locations the left and right knee of each subject.

		Left knee			**Right knee**		
		x	*y*	*z*	*x*	*y*	*z* [a]
Subject 1	MB (mm)	0	-456.83	0	0	-488.3	0
	FC (mm)	-2.09	-464.1	0	11.06	-479.2	0
	Difference (mm) [b]	*7.56*			*14.32*		
	FC knee axis [c] (deg.)	-5.67	-5.94	-0.3	6.75	-1.07	0.06
	FC axis angle [d] (deg.)	8.20			6.83		
	Knee translation (mm)[e]	53.57	21.3	0	53.26	21.1	0
Subject 2	MB (mm)	0	-419.51	0	0	-434.22	0
	FC (mm)	-55.92	-423.74	0	29.66	-395.69	0
	Difference (mm)	*56.08*			*48.65*		
	FC knee axis (deg.)	-11.49	-17.42	-1.77	3.76	7.43	-0.24
	FC axis angle (deg.)	20.77			8.32		
	Knee translation (mm)	-11.64	-15.7	0	-0.13	16.2	0
Subject 3	MB (mm)	0	-402.74	0	0	-423.58	0
	FC (mm)	-49.72	-388.53	0	-53.74	-422.9	0
	Difference (mm)	*51.71*			*53.74*		
	FC knee axis (deg.)	-8.73	-11.40	-0.87	10.05	25.38	-2.27
	FC axis angle (deg.)	14.32			27.17		
	Knee translation (mm)	-25.65	20.9	0	-26.93	2.7	0
			x		*y*		*z*
Mean [f]	MB (mm)		0		-437.53 ± 30.63		0
	FC (mm)		33.70 ± 23.15		-429.03 ± 36.23		0
	Difference (mm)				*38.68 ± 21.73*		
	FC knee axis (deg.)		4.70 ± 4.28		5.23 ± 6.72		0.71 ± 0.64
	FC axis angle (deg.)				14.23±8.20		
	Knee translation (mm)		28.53 ± 16.32		21.64 ± 7.13		0

[a] *All data is presented in femur coordinate system: x-axis pointing forward, y-axis pointing upward, z-axis pointing to the right.*
[b] *Global distance between MB and FC knee joint location.*
[c] *Cartesian angles.*
[d] *Euclidian angle.*
[e] *Knee translation is the translation of the IHA occurring from 0 to 40 degrees of loaded knee flexion.*
[f] *Mean angles and translation are calculated with absolute values.*

3.1.3 Segment lengths

Segment lengths as a result of scaling with MB or FC joint centres are presented in Table 4. It can be seen that the differences in segment lengths are smaller than the distances between MB and FC joint centres as presented in the previous sections 3.1.1 and 3.1.2.

Table 4. *Segment lengths*
MB and FC based segments lengths

		Pelvis	Right femur	Left femur	Right tibia	Left tibia
Subject 1	**MB (mm)**	208.37	456.83	488.3	471.2	465.39
	FC (mm)	189.36	464.1	479.33	463.75	477.14
	Difference (mm)	*19.01*	*-7.27*	*8.97*	*7.45*	*-11.75*
Subject 2	**MB (mm)**	188.46	419.51	434.23	383.62	369.38
	FC (mm)	173.43	427.41	396.78	384.53	407.39
	Difference (mm)	*15.03*	*-7.90*	*37.45*	*-0.91*	*-38.02*
Subject 3	**MB (mm)**	191.74	402.74	423.58	370.69	378.11
	FC (mm)	193.86	391.70	426.30	390.43	395.58
	Difference (mm)	*2.38*	*11.04*	*-2.72*	*-19.75*	*-17.47*
		Pelvis		*Femur*		*Tibia*
Mean	**MB (mm)**	196.19 ± 10.67		437.53 ± 30.63		406.40 ± 48.26
	FC (mm)	185.55 ± 10.73		430.94 ± 35.16		419.80 ± 40.17
	Difference (mm) [a]	*12.14 ± 8.68*		*12.56 ± 12.50*		*15.89 ± 12.81*

[a] *Mean differences are calculated with absolute values.*

3.2 MT length and velocity

Figure 6 shows the MT lengths and velocities of the selected muscles during UI gait as a result of MB and FC calibration for the right leg of each subject. In a similar way Figure 7 gives an overview of the MT lengths and velocities associated with the KF and SK models. Mean peak MT length and velocity differences of the FC and SK models can be found in Tables 5 and 6. A comprehensive overview of each subject can be found in Appendix F | Muscle-tendon outcome.

3.2.1 Effect of calibration methods

Overall it can be seen that calibration methods have most effect on peak MT lengths and to a lesser extend on peak MT velocities. This implies that the MT length curve is mostly shifted up or down as a result of the different calibration methods without clearly changing the shape of the curve. Differences as a result of functional calibration methods varied up to 27.6% for peak MT length and up to 17.0% for peak MT velocities.
Hip joint calibration has most effect on semimembranosus and rectus femoris muscle lengths with a maximum mean difference of 12.5% between the MB and HF models. The effect of hip joint calibration on MT velocities was most visible for the psoas muscle with a mean difference of 6.6%.

The effect of knee calibration on MT length is small for all studied muscles. The maximum mean MT peak difference for the gastrocnemius muscle is 3.7%. Knee calibration also had a limited effect on MT velocities with differences smaller than 3%. Only gastrocnemius MT velocity was slightly more affected with a mean difference of 6.4%.
The combined hip and knee joint calibration had a relatively large effect on all MT lengths. The largest mean difference in MT length was 17.1% for the psoas muscle. Also the effect on MT velocity was relatively large for the psoas and gastrocnemius muscle, with a maximum of 9.9%.

3.2.2 Effect of knee translation

Knee translation has a small effect on peak MT length, but does affect peak MT velocity in sway phase. Knee translation affects the slope of the MT length curve in sway phase, resulting in a small effect on MT peak length, but an enlarged effect on peak MT velocity. Differences in peak MT length ranged up to 3.4% and up to 26.0% for MT velocity. Evidently, the effect of knee translation is only present for muscles crossing the knee joint; therefore no effect on the psoas muscles is noticed.
The KF-D model has most effect on the semimembranosus muscle for which a mean peak MT velocity difference of 16.9% was found. Rectus femoris and gastrocnemius peak MT velocities were also affected by adding the knee translation of Delp with mean differences of 10.9% and 7.6%.
Compared to the KF-D model, the KF-S model has less effect on the semimembranosus muscles, but slightly more for rectus femoris and gastrocnemius muscles. The biggest differences found in peak MT velocity for semimembranosus, rectus femoris and gastrocnemius muscles were respectively 1.8%, 18.9% and 16.0%.

3.2.3 UI versus CP gait data

Overall the effect of different models on MT length are comparable for unimpaired and CP gait. The effect on MT velocities is smaller for CP gait, which can be reasoned because angular velocities of the segments are lower during typical stiff CP gait. Also the walking speed in this study was set slower for CP gait.

***Table 5**. Effect on MT length*
Effect of FC and KT on muscle-tendon length for UI and CP gait. Mean peak MT length differences in of the psoas, semimembranosus, rectus femoris and gastrocnemius muscle of FC models compared to peak MT length of MB model in and peak data of SK models are compared to of the KF model.

			Psoas		Semimem.		Rect. Fem.		Gastroc.		Average
			%	*SD*	%	*SD*	%	*SD*	%	*SD*	%
UI	**FC**	**HF**	2.37	*± 1.68*	12.48	*± 5.93*	10.73	*± 4.13*	0.17	*± 0.07*	6.44
		KF	1.09	*± 0.64*	2.19	*± 1.17*	2.50	*± 1.63*	3.61	*± 1.53*	2.35
		HKF	15.33	*± 12.16*	8.62	*± 7.54*	4.39	*± 2.50*	6.44	*± 6.65*	8.70
	SK	**KF-D**	0.02	*± 0.04*	0.05	*± 0.03*	0.28	*± 1.00*	0.02	*± 0.02*	0.09
		KF-S	0.06	*± 0.03*	0.03	*± 0.00*	0.25	*± 0.07*	0.05	*± 0.01*	0.10
CP	**FC**	**HF**	1.96	*± 1.72*	12.09	*± 7.94*	9.18	*± 5.82*	0.33	*± 0.20*	5.89
		KF	1.46	*± 0.86*	2.98	*± 1.82*	3.16	*± 2.28*	3.41	*± 2.24*	2.75
		HKF	17.08	*± 12.62*	8.54	*± 8.32*	3.33	*± 3.07*	7.60	*± 7.51*	9.14
	SK	**KF-D**	0.05	*± 0.02*	0.47	*± 0.56*	1.50	*± 1.27*	0.10	*± 0.09*	0.53
		KF-S	0.05	*± 0.09*	0.58	*± 0.72*	0.80	*± 0.99*	0.16	*± 0.03*	0.40

***Table 6.** Effect on MT velocity*
Effect FC and KT on muscle-tendon velocity for UI and CP gait.. Mean peak MT velocity differences in of the psoas, semimembranosus, rectus femoris and gastrocnemius muscle of FC models compared to peak MT velocity of MB model in and peak velocity of SK models compared to peak velocity of KF model.

			Psoas		Semimem.		Rect. Fem.		Gastroc.		Average
			%	*SD*	%	*SD*	%	*SD*	%	*SD*	%
UI	**FC**	**HF**	6.57	*± 1.98*	2.39	*± 4.24*	0.87	*± 1.25*	2.34	*± 2.31*	3.04
		KF	2.13	*± 2.03*	2.79	*± 2.23*	1.04	*± 0.71*	6.37	*± 5.13*	3.08
		HKF	9.85	*± 5.94*	1.77	*± 1.11*	2.50	*± 2.19*	3.65	*± 3.81*	4.44
	SK	**KF-D**	0.65	± 0.42	16.85	± 4.95	10.89	± 5.09	7.11	± 3.73	8.87
		KF-S	0.9	± 0.95	6.84	± 2.85	12.97	± 4.69	9.32	± 4.55	7.51
CP	**FC**	**HF**	2.35	*± 2.47*	0.79	*± 0.60*	1.51	*± 1.95*	0.88	*± 0.67*	1.38
		KF	1.59	*± 0.87*	2.93	*± 2.07*	1.52	*± 0.86*	1.71	*± 1.29*	1.94
		HKF	2.66	*± 2.19*	2.40	*± 1.14*	3.21	*± 3.31*	0.77	*± 0.46*	2.26
	SK	**KF-D**	0.60	± 0.15	16.33	± 6.45	6.90	± 4.49	7.62	± 3.71	7.86
		KF-S	0.99	± 0.89	0.73	± 0.76	1.95	± 2.64	10.74	± 3.76	3.60

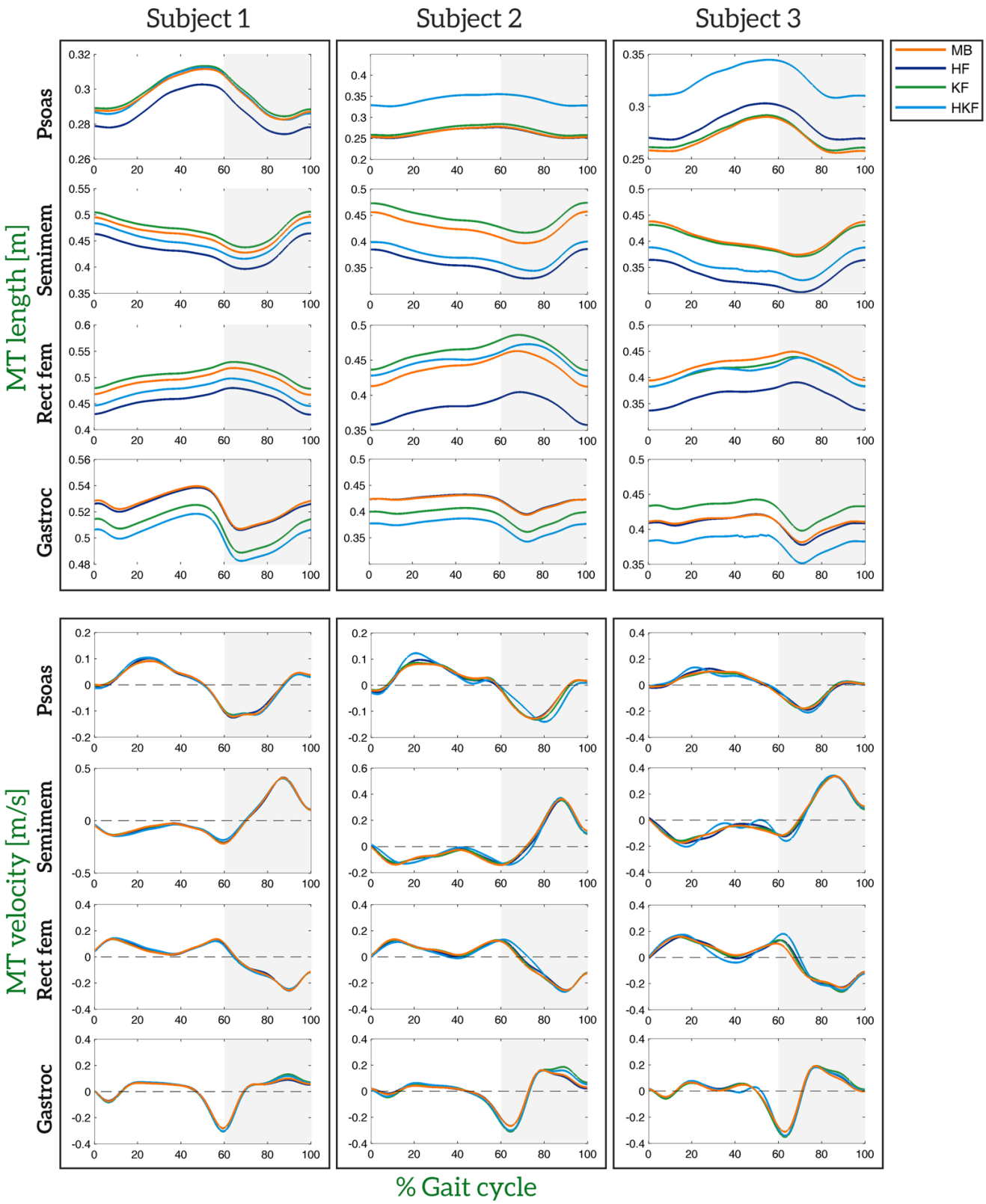

Figure 6. *MT length and velocity MB and FC models*
MT length and velocities of MB and FC models of the right leg of each subject associated with UI gait data.

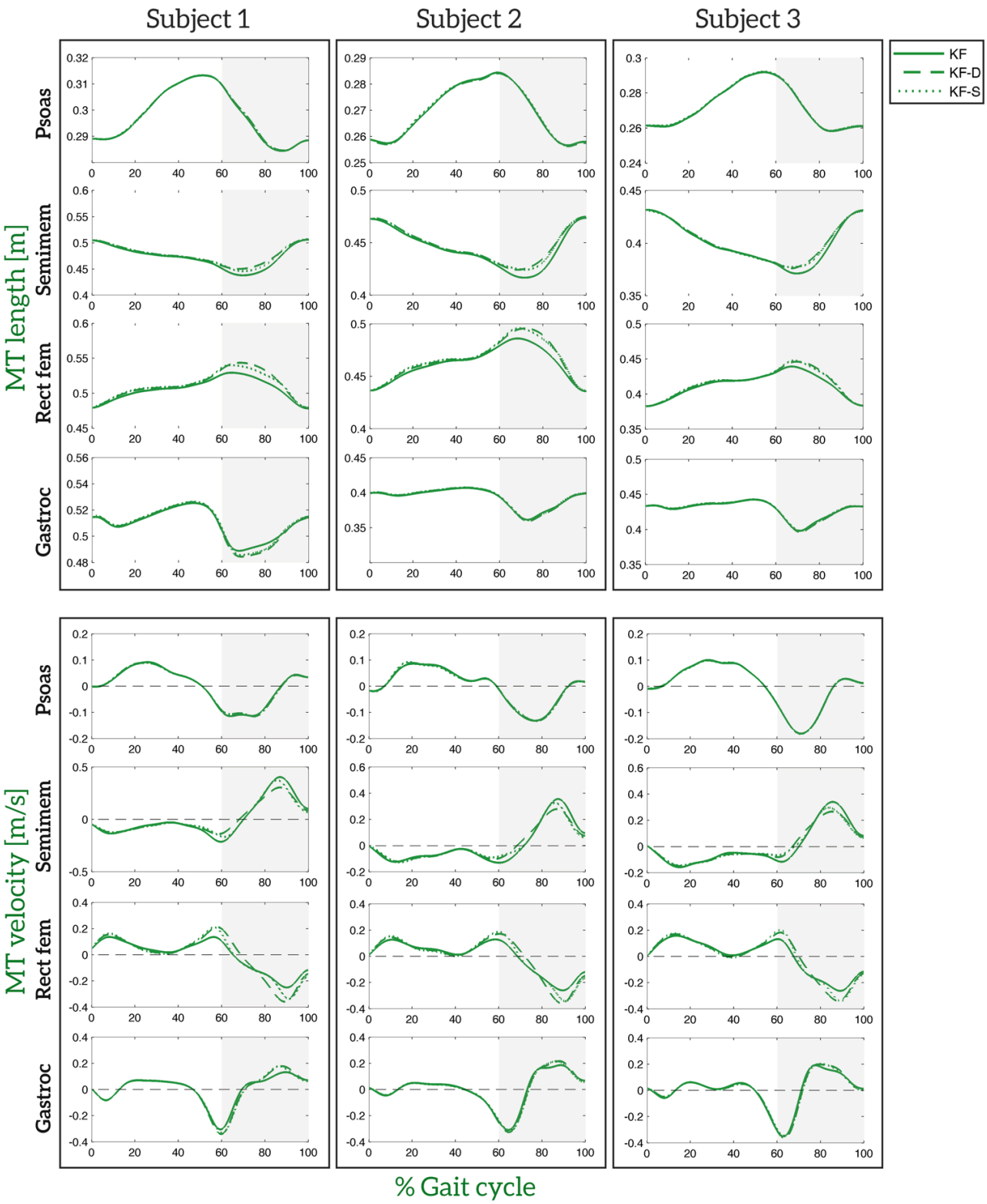

Figure 7. *MT length and velocity KF and SK models*
MT length and velocities of KF and SK models of the right leg of each subject associated with UI gait data.

3.2.4 Effect on clinical decision-making

The MT length and velocity curves of each muscle during CP gait were evaluated with the six different models as discussed in section 2.5 to determine whether a muscle would be classified as too short or too slow. Figure 8 shows the MT length curves of the semimembranosus muscle and the MT velocity curves of the gastrocnemius muscle of a typical subject estimated with the different models. The curves associated with CP gait are plotted together with the average UI data. It can be seen that the semimembranosus peak MT length estimation of the HF and HKF models would be considered within the average range whereas the MB model would classify this muscle as too short. Evaluation of muscle behaviour for each subject estimated with the different models led to a total of 24 clinical decisions based on MT length and 24 based on MT velocity that were compared to the decisions based on the MB models of each subject (Table 7).

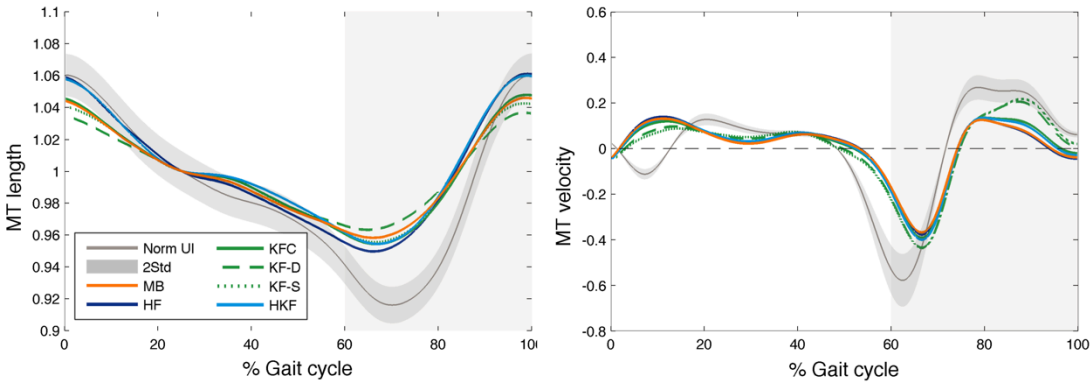

Figure 8. *Effect on clinical decision-making*
MT length and velocity curves of CP gait compared with average UI gait data (grey line) plus or minus two times the SD (shaded area), as a guideline for clinical decision-making. Left: Semimembranosus MT length of the right leg of PP3. Clinical decision based on HF and HKF differs from MB. Right: Gastrocnemius MT velocity of the right leg of PP1. Clinical decision based on KF-D and KF-S differs from MB.

All models led to at least one different clinical decision out of the 24, compared to the MB model based decision. The combined functionally calibrated hip and knee model does affect velocity-based decisions strongly. Respectively 6 and 4 out of 24 decisions based on the KF-D and KF-S model, differentiate from the MB model based decisions.

Table 7. *Number of different clinical decisions*
Number of clinical decisions based on FC and SK models that differ from those based on MB models

		FC models			**SK models**	
		HF	KF	HKF	KF-D	KF-S
MT Length	**Psoas**	0	1	2	1	1
	Semimem.[a]	1	0	2	1	0
	Rect. Fem.[b]	0	0	0	1	0
	Gastroc.[c]	0	0	0	0	0
	Total	*1*	*1*	*4*	*3*	*1*
MT Velocity	**Psoas**	0	0	0	0	0
	Semimem.[a]	1	0	1	2	0
	Rect. Fem.[b]	0	0	0	0	0
	Gastroc.[c]	0	1	1	4	4
	Total	*1*	*1*	*2*	*6*	*4*

[a] *Semimembranosus muscle,* [b] *rectus femoris muscle,* [c] *gastrocnemius muscle*

4 DISCUSSION

Analysis of muscle-tendon lengths and velocities may help to distinguish individuals who have too short or too slow muscles from those who do not. Hence musculoskeletal modelling can be of great assistance in predicting the effect and necessity of surgical tendon lengthening in CP patients. However generic MS models do not represent bone deformities that are often present in CP patients. It is not known how variations in MS geometry affect the accuracy of MT length estimations. This study aimed on providing more insight in to the effect of differences in MS geometry in terms of joint locations and orientations relative to anatomical landmarks on MT length and velocity. It was shown that functional calibration of joint coordinate systems in healthy subjects already results in large differences compared to the locations in the generically scaled model. Although no CP patients were tested in this research it can be reasoned that the effect will only be larger for subjects with severe bone deformities.

Because no MR-imaging techniques were used in this study *true* joint centres are not known and neither are the true axes of rotation. For this reason only a difference between MB- and FC-based joint coordinate systems can be presented. Other studies have tested the accuracy of the calibration methods used, which provides more insight in the accuracy of the joint centres estimations provided in this study.

Functional hip joint calibration with the use of a sphere fit methods can reach an accuracy of 3 mm when a spherical range of motion of 45° was carried out [20]. Maximum hip angles performed in the FC trial were about 40°, which might have influenced the accuracy of the estimated hip joint angles found in this study. One trial led to a clearly unrealistic joint centre location, which might be due to a combination of limited hip flexion angles, noisy marker data and skin movement artefacts. The mean differences between the MB and FC hip joint centres were larger than the differences found by Leardini, et al. [11]. This can be explained because Leardini only used male subjects in his study and the largest differences found in this study were associated with the female subjects. This indicates that the proportions of the generic model, based on male anthropomorphic measurements do not very well represent female proportions of the pelvis.

Root mean square errors of the knee joint axes estimated with the IHA method are largely depending on the amount of noise on the marker data and the exerted flexion angle of the knee. Ehrig, et al. [21] found a maximum root mean square error of 36 mm when marker data associated with knee flexion angles up to 90° were used and skin movement artefacts were simulated with Gaussian noise with a standard deviation of 10 mm. To reduce the effect of noise, the marker data in this study was filtered with a second order Butterworth filter and the data corresponding to low angular velocities were not used for the calculation of the IHA. However, in some subjects the IHA estimations still appeared to be influenced by noise, which can be seen in the rather random projections of the IHA on the midplane between the epicondyles in some subjects (Appendix C2.2 | Functional knee joint calibration). The differences in the joint locations between the MB- and FC-based knee axes might therefore be overestimated, even though the differences are comparable to the findings of Chin, et al. [22]. They compared an anatomically based estimation of the elbow axis of rotation with a

functionally based method using finite helical axis and found a difference in joint location of 38.9 ± 24.3 mm, whereas the mean differences for the knee axis locations in this study were 38.7 ± 21.7 mm. The mean rotation angle between the MB and FC axes was a bit smaller in the study of Chin compared to the findings in this study, 7.4° ± 4.5° against 14.0° ± 8.5°.

Both functional hip and knee calibration methods can reach better accuracy in healthy subjects than regression based methods when executed carefully [11] and was found to be better repeatable [23]. Another advantage of functional calibration is that accurate positioning of markers on the ALs is not needed when the same position of the markers is maintained throughout the calibration and gait trials. This makes FC better suitable for CP patients where ALs are often not easy to palpate.

A side step in calibrating joint coordinate systems was made by looking at the effect of knee translation. The knee translation described by Delp was modified in attempt to make the knee translation curve more applicable for gait. However this modification was not based on experimental data. Since the effect of knee translation was shown to be substantial, further research is needed to accurately describe the knee translation curve associated with gait. Considering the large effect of knee translation on MT length and velocity in healthy subjects, it would even be advisable to develop a pathology-based method to describe knee translation curves when studying MT length and velocity of patients with bone deformities.

The scaling of the segments was done along the anatomical axes. Because the segments were not deformed otherwise, a compromise between modelling the exact locations of the joints or the ALs had to be made. By giving priority to accurate locations of the joints this sometimes led to non-realistic positions of the ALs relative to the joint centres. Because experimental markers were used in inverse kinematics to simulate gait instead of joint centre locations this led to abnormal joint kinematics in some subjects (Appendix D | Kinematics). This effect was most visible in the HKF models where both hip and knee joints were determined functionally. For future research a deformable MS model that can match segmental proportions to both joint centres and ALs would be advisable for more accurate results.

Because this study focuses on the effect of calibration methods on MT lengths and velocities, the effect on joint kinematics and kinetics is not explained, but can be found Appendix D | Kinematics and Appendix E | Kinetics.

Calibration methods seem to have little effect on absolute MT lengths and slightly more effect on MT velocities. However these small differences as a result of different calibration methods sometimes led to other clinical decisions. Therefore model output differences must be compared with the threshold above or below a clinical decision is altered to evaluate whether these values are critical. Although the impact of calibration methods on clinical decision-making seems to be substantial, the results presented in this study are based on mimicked CP gait of only 3 subjects. Therefore these results only have an illustrative purpose to indicate the need of further research in accurate joint calibration and scaling techniques.

5 CONCLUSION

The effect of different calibration methods on joint coordinate systems and MT outcomes was studied. Joint calibration methods have a large effect on joint coordinate systems in healthy subjects, with a presumably even more present effect in CP patients with severe bone deformities.

The effect of joint calibration methods on MT length and velocity was found to be small. Due to the relatively long muscles in the lower extremity the relative differences in MT length as a result of differences in joint coordinate systems were found to be small. Also the shapes of the MT length curves were not altered much, resulting in a small effect on MT velocities.

Functional calibration of the knee joint showed the existence of knee translation during the stance phase in gait. Modelling knee translation does alter the shape of the MT length curve and therefore affects MT velocity. Further research is needed in developing gait-specific knee translation curves of healthy subjects and CP patients to better understand the influence of modelling knee translation.

Although the effect of different calibration methods on MT length and velocity is small, it was found to be large enough to potentially alter clinical decision-making. The influence of joint calibration methods should therefore be kept in mind when making modelling decisions or evaluating MS model outcome.

6 GLOSSARY

List of acronyms and abbreviations

AL	Anatomical landmark
CP	Cerebral Palsy
FC	Functional calibration
HF	Functional hip
HKF	Functional hip and knee
IHA	Instantaneous helical axis
KF	Functional knee
KF-D	Functional knee with Delp translation
KF-S	Functional knee with translation in stance phase
MB	Marker-based
MS	Musculoskeletal
MT	Muscle-tendon
SD	Standard deviation
SK	Knee translation
UI	Unimpaired

7 REFERENCES

[1] F. Stanley, E. Blair, and E. Alberman, *Cerebral palsies: epidemiology and causal pathways*: Cambridge University Press, 2000.

[2] S. L. Delp, A. S. Arnold, R. A. Speers, and C. A. Moore, "Hamstrings and psoas lengths during normal and crouch gait: Implications for muscle-tendon surgery," *Journal of Orthopaedic Research,* vol. 14, pp. 144-151, 1996.

[3] D. Borton, K. Walker, M. Pirpiris, G. Nattrass, and H. Graham, "Isolated calf lengthening in cerebral palsy OUTCOME ANALYSIS OF RISK FACTORS," *Journal of Bone & Joint Surgery, British Volume,* vol. 83, pp. 364-370, 2001.

[4] H. K. Graham and J. Fixsen, "Lengthening of the calcaneal tendon in spastic hemiplegia by the White slide technique. A long-term review," *Journal of Bone & Joint Surgery, British Volume,* vol. 70, pp. 472-475, 1988.

[5] P. A. DeLuca, S. Õunpuu, R. B. Davis, and J. H. P. Walsh, "Effect of Hamstring and Psoas Lengthening on Pelvic Tilt in Patients with Spastic Diplegic Cerebral Palsy," *Journal of Pediatric Orthopaedics,* vol. 18, 1998.

[6] A. S. Arnold, M. Q. Liu, M. H. Schwartz, S. Õunpuu, L. S. Dias, and S. L. Delp, "Do the hamstrings operate at increased muscle–tendon lengths and velocities after surgical lengthening?," *Journal of Biomechanics,* vol. 39, pp. 1498-1506, // 2006.

[7] A. S. Arnold, M. Q. Liu, M. H. Schwartz, S. Ounpuu, and S. L. Delp, "The role of estimating muscle-tendon lengths and velocities of the hamstrings in the evaluation and treatment of crouch gait," *Gait & posture,* vol. 23, pp. 273-281, 2006.

[8] A. Arnold, S. Blemker, and S. Delp, "Evaluation of a Deformable Musculoskeletal Model for Estimating Muscle–Tendon Lengths During Crouch Gait," *Annals of Biomedical Engineering,* vol. 29, pp. 263-274, 2001/03/01 2001.

[9] A. L. Bell, R. A. Brand, and D. R. Pedersen, "Prediction of hip joint centre location from external landmarks," *Human Movement Science,* vol. 8, pp. 3-16, 1989.

[10] D. A. Bruening, A. N. Crewe, and F. L. Buczek, "A simple, anatomically based correction to the conventional ankle joint center," *Clinical Biomechanics,* vol. 23, pp. 1299-1302, 12// 2008.

[11] A. Leardini, A. Cappozzo, F. Catani, S. Toksvig-Larsen, A. Petitto, V. Sforza*, et al.*, "Validation of a functional method for the estimation of hip joint centre location," *Journal of Biomechanics,* vol. 32, pp. 99-103, 1// 1999.

[12] W. His, *Die anatomische Nomenclatur. Nomina anatomica: Verzeichniss der von der anatomischen Gesellschaft auf ihrer IX. Versammlung in Basel angenommenen Namen*: Veit & Company, 1895.

[13] T. v. d. Bogert, "Human Body Model Reference Manual," Motek Medical B.V.2011.

[14] H. J. Woltring, "Biomechanics of Human Movement, Applications in Rehabilitation, Sport and Ergonomics," *Biomechanics of Human Movement, Applications in Rehabilitation, Sport and Ergonomics,* pp. 203-237, 1990.

[15] L. Blankevoort, R. Huiskes, and A. De Lange, "Helical axes of passive knee joint motions," *Journal of Biomechanics,* vol. 23, pp. 1219-1229, // 1990.

[16] S. L. Delp, J. P. Loan, M. G. Hoy, F. E. Zajac, E. L. Topp, and J. M. Rosen, "An interactive graphics-based model of the lower extremity to study orthopaedic surgical procedures," *Biomedical Engineering, IEEE Transactions on,* vol. 37, pp. 757-767, 1990.

[17] S. L. Delp, F. C. Anderson, A. S. Arnold, P. Loan, A. Habib, C. T. John*, et al.*, "OpenSim: open-source software to create and analyze dynamic simulations of movement," *Biomedical Engineering, IEEE Transactions on,* vol. 54, pp. 1940-1950, 2007.

[18] V. T. Inman, H. J. Ralston, and F. Todd, *Human walking*: Williams & Wilkins, 1981.

[19] N. Thompson, R. Baker, A. Cosgrove, I. Corry, and H. Graham, "Musculoskeletal modelling in determining the effect of botulinum toxin on the hamstrings of patients with crouch gait," *Developmental Medicine & Child Neurology,* vol. 40, pp. 622-625, 1998.

[20] R. M. Ehrig, W. R. Taylor, G. N. Duda, and M. O. Heller, "A survey of formal methods for determining the centre of rotation of ball joints," *Journal of biomechanics,* vol. 39, pp. 2798-2809, 2006.

[21] R. M. Ehrig, W. R. Taylor, G. N. Duda, and M. O. Heller, "A survey of formal methods for determining functional joint axes," *Journal of biomechanics,* vol. 40, pp. 2150-2157, 2007.

[22] A. Chin, D. Lloyd, J. Alderson, B. Elliott, and P. Mills, "A marker-based mean finite helical axis model to determine elbow rotation axes and kinematics in vivo," *Journal of applied biomechanics,* vol. 26, 2010.

[23] T. F. Besier, D. L. Sturnieks, J. A. Alderson, and D. G. Lloyd, "Repeatability of gait data using a functional hip joint centre and a mean helical knee axis," *Journal of Biomechanics,* vol. 36, pp. 1159-1168, 8// 2003.

[24] F. M. Griffin, J. N. Insall, and G. R. Scuderi, "The posterior condylar angle in osteoarthritic knees," *The Journal of Arthroplasty,* vol. 13, pp. 812-815, 10// 1998.

8 APPENDICES

Appendix A Equipment

Appendix A.1 Straps for mimicking CP gait

Figure 9 shows the straps that were attached to the waist and ankles of the subjects to restrict knee flexion in mimicking CP gait.

Figure 9. *Straps to restrict knee flexion*

Appendix A.2 GRAIL

Figure 10 shows the GRAIL motion capture system. GRAIL consists of an instrumented dual-belt treadmill, an integrated motion-capture system and 3 video cameras.
Motion cameras are used to track the experimental markers attached to the subjects in time. Video cameras record the session to compare and check the marker data with the real motion. Desired speed, acceleration and length of the gait trail can be fed to the instrumented treadmill.

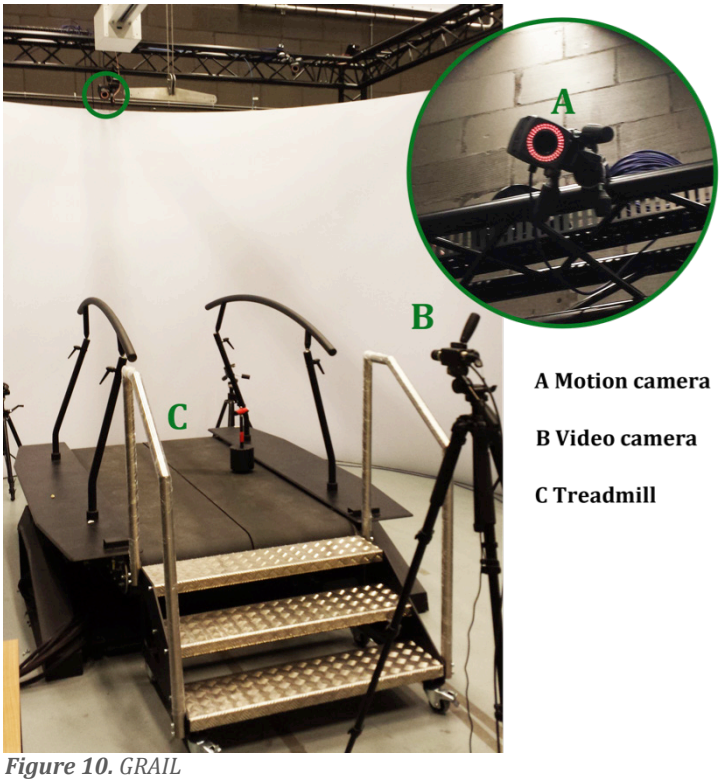

Figure 10. *GRAIL*

Appendix B Lower extremity marker set

Figure 11 shows the experimental markers that were used during the motion capturing trials and the virtual markers that where allocated on the same locations on the MS model.

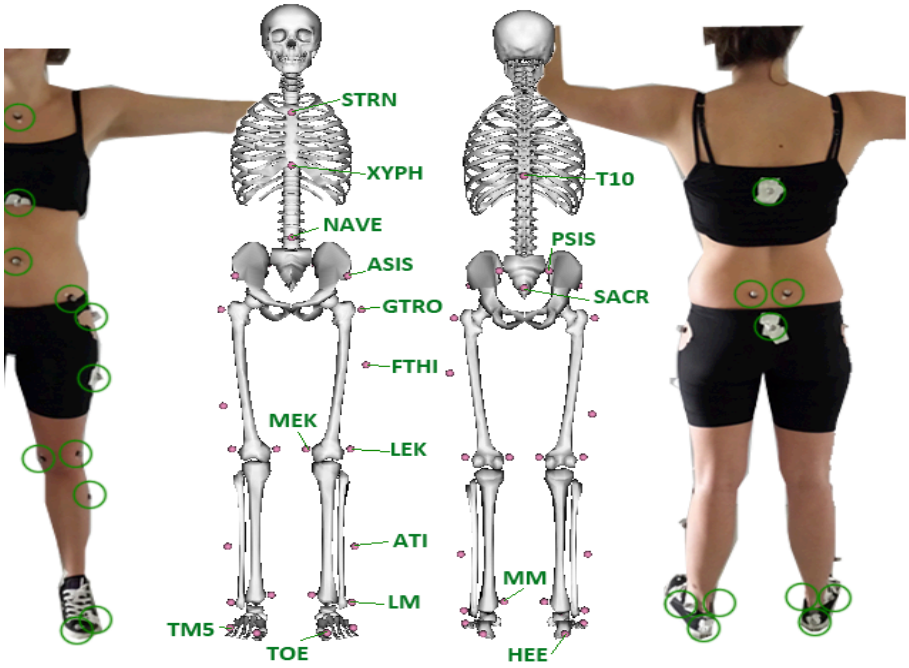

Figure 11. *Experimental and virtual marker set*

Table 8 clarifies the names and locations of the markers.

Table 8. *Marker names and location*

Name	Anatomical location
STRN	Top of sternum
T10	Tenth thoracic vertebra
XYPH	Xyphoid process (bottom of sternum)
NAVE	Navel
SACR	Sacrum
LASIS	Left anterior superior iliac spine
RASIS	Right anterior superior iliac spine
LPSIS	Left posterior superior iliac spine
RPSIS	Right posterior superior iliac spine
LGTRO	Left greater trochanter
RGTRO	Right greater trochanter
FLTHI	Left lateral side of femur
FRTHI	Right lateral side of femur
LLEK	Left lateral epicondyle of the knee
LMEK	Left medial epicondyle of the knee
RLEK	Right lateral epicondyle of the knee
RMEK	Left medial epicondyle of the knee
LATI	Left lateral side of tibia
RATI	Right lateral side of tibia
LLM	Left lateral malleolus
LMM	Left medial malleolus
RLM	Right lateral malleolus
RMM	Right medial malleolus
RHEE	Right heel
LHEE	Left heel
RTOE	Right second toe
LTOE	Left second toe
RMT5	Right head of 5th metatarsal
LMT5	Left head of 5th metatarsal

Remarks

Markers were placed by a researcher with limited physical knowledge. This might have led to inaccurate anatomical landmark palpation and marker placement.

Appendix C Joint calibration

Appendix C.1 Hip joint calibration

This appendix describes both regression based and functional hip joint calibration. Joint centre locations will be presented in the local reference frame of the pelvis as defined in figure 12.

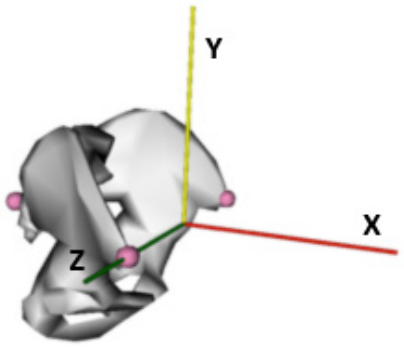

Figure 12. *Pelvis coordinate system*
Origin: *Midpoint between LASIS and RASIS marker*
Z-axis: *Pointing from origin to RASIS marker*
Y-axis: *Perpendicular to the plane LASIS-RASIS-SACR*
X-axis: *Perpendicular to Z- and Y-axis*

Appendix C1.1 Marker-based hip joint calibration

Marker based hip joint centres are estimated with a algorithm proposed by Bell, et al. [9] (fig. 13):
X-axis location: x-axis location of greater trochanter marker
Y-axis location: z-axis location of ASIS -0.3 D* in z-direction
Z-axis location: y-axis location of ASIS ± 0.14 D in y-direction.
*With D: the distance between the left and right anterior superior iliac spines (ASIS).

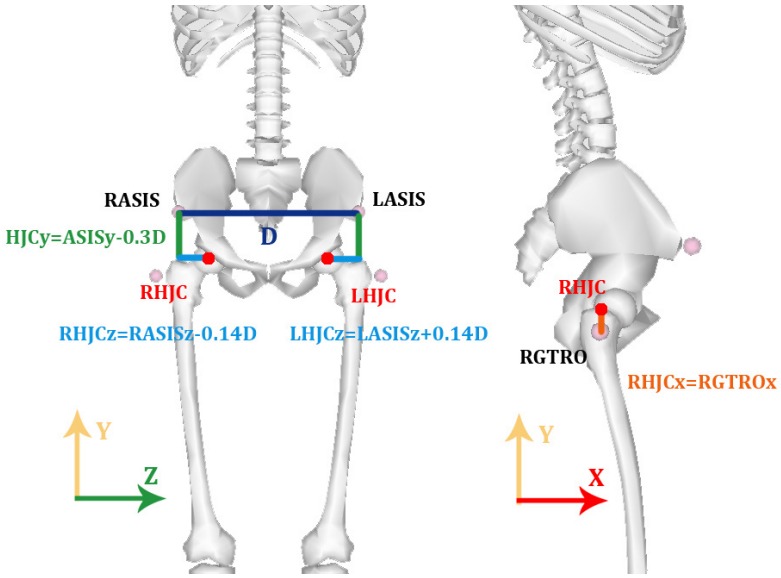

Figure 13. *Marker-based hip joint calibration*
Regression based hip joint centre estimation proposed by Bell.

Appendix C1.2 | Functional hip joint calibration

Functional hip joint centres were estimated with the use of a least square sphere fit approach. By finding the least square sphere fit of the trajectory of the femur relative to the pelvis the hip joint centre can be estimated (figure 15). For the description of the femur motion the midpoint p_i between the medial and lateral markers of the epicondyles was taken. By minimizing the EQ. 1 the hip joint centre can be estimated.

$$f(x_c, y, z_c, r) = \frac{1}{n}\sum_{i=1}^{n} \left|\sqrt{(x_i - x_c)^2 + (y_i - y_c)^2 + (z_i - z_c)^2} - r\right| \quad (1)$$

With r representing the radius of the sphere and x_i, y_i, z_i represent the coordinates of p_i at time frame i over a total of n frames.
Marker trajectories needed for hip joint estimation were transformed into the pelvic reference frame via simple matrix transformations (Eq. 2).

$$p_{local} = inv(R) \cdot (p_{global} - p_{origin\ pelvis\ global}) \quad (2)$$

p_{global} are the global marker trajectories and p_{local} are the transformed marker trajectories in the local reference frame of the pelvis. Orientation matrix R was obtained by defining the unit direction vectors of the local pelvic reference frame axes (Eq. 3-6)

$$z = |RASIS - LASIS| \quad (3)$$
$$y = |(SACR - LASIS) \times z| \quad (4)$$
$$x = |y \times x| \quad (5)$$
$$R = [x\ y\ z] \quad (6)$$

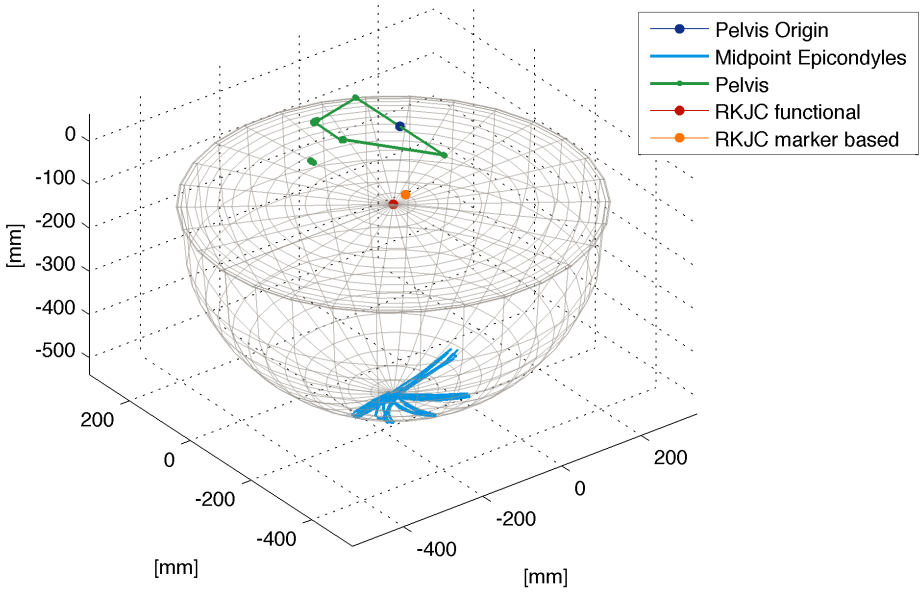

Figure 14. *Functional hip joint calibration*

Appendix C2 Knee joint calibration

Appendix C2.1 Marker-based knee joint calibration

The marker-based knee joint axis of rotation is taken to be the line between the medial and lateral epicondyles of the knee. The centre of the knee joint is defined as the midpoint of the knee axis of rotation (Figure 15).

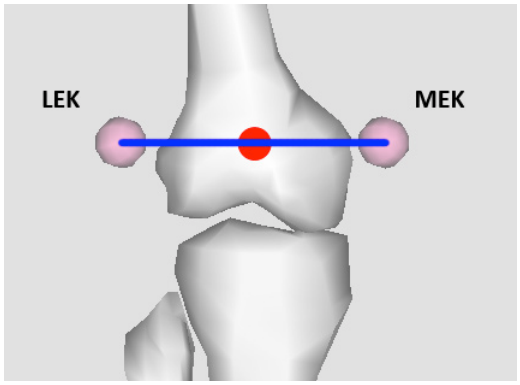

Figure 15. *Marker-based knee joint calibration*
Marker based knee joint centre (red dot) and axis of rotation (blue line)

Appendix C2.2 Functional knee joint calibration

The functional rotation axis of the knee is estimated with the use if the instantaneous helical axis (IHA) method [14]. The IHA is the line about and along which one segment is instananeously moving with respect to the other segment. For the calculation of the IHA of the knee the movement of the tibia is described with respect to the femur. Therefore the marker trajectories belonging to the tibia segment are transformed into the femur local reference frame as was done for the pelvis local reference frame in the previous section with local reference frames as defined in figure 16.

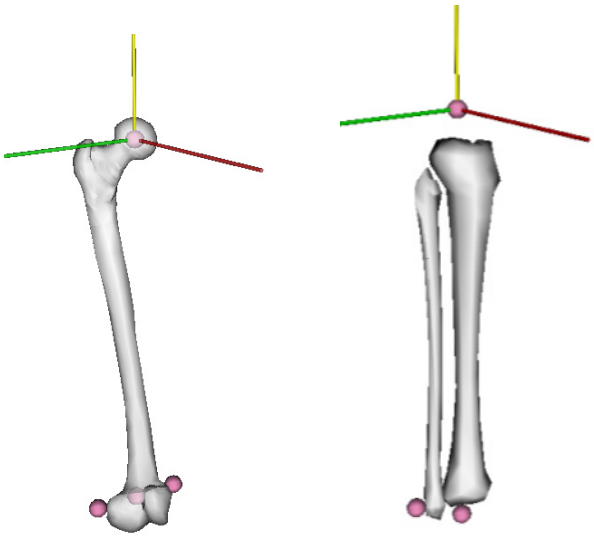

Femur (left)
Origin: Centre of femoral head
Y-axis: Pointing upward from knee joint centre (KJC) to hip joint centre (HJC)
X-axis: Perpendicular to the plane KJC-HJC-LEK (lateral epicondyle)
Y-axis: Perpendicular to X- and Y-axis

Tibia (right)
Origin: Knee joint centre
Y-axis: Pointing upward from ankle joint centre (AJC) to knee joint centre (KJC)
X-axis: Perpendicular to the plane AJC-KJC-LM (lateral malleolus)
Y-axis: Perpendicular to X- and Y-axis

Figure 16. *Femur and tibia coordinate systems*

Calculation of IHA

In order to describe an instantaneous helical axis the direction vector, a point in space through which the axis is passing and a translation vector along the axis must be known. The direction vector of the IHA is found to be parallel with the angular velocity vector. Angular velocity can be calculated when the orientation matrix R is known over time. Given the orientation matrix R, the angular velocity tensor W can be obtained by Eq. 1-2.

$$\frac{dR(t)}{dt} = W(t) \cdot R(t) \quad (1)$$

$$W(t) = \frac{dA(t)}{dt} \cdot R^{-1}(t) \quad (2)$$

The angular velocity ω =[$\omega_x\ \omega_y\ \omega_z$] can then be retrieved from $W(t) = \begin{bmatrix} 0 & -\omega_{z(t)} & \omega_{y(t)} \\ \omega_{z(t)} & 0 & -\omega_{x(t)} \\ -\omega_{y(t)} & \omega_{x(t)} & 0 \end{bmatrix}$.

The direction of the IHA is described by the unit vector of the angular velocity $D_{IHA} = \frac{\omega}{|\omega|}$

The projection of point P on the IHA can than be described by the following equation:

$$P_{IHA} = P + \frac{\omega \times \frac{dP}{d(t)}}{|\omega|^2} \quad (3)$$

and the instantaneous velocity that describes the translation along the IHA can be calculated by the formula:

$$V_{IHA} = \frac{dP}{d(t)} \cdot D_{IHA} \quad (4)$$

IHA of loaded and unloaded knee

To illustrate the differences of the IHA between the loaded and unloaded knee the results of the left leg of subject 1 are shown. Figure 17 shows the projection of the IHA in space seen in the local reference frame of the femur for the loaded and unloaded knee.

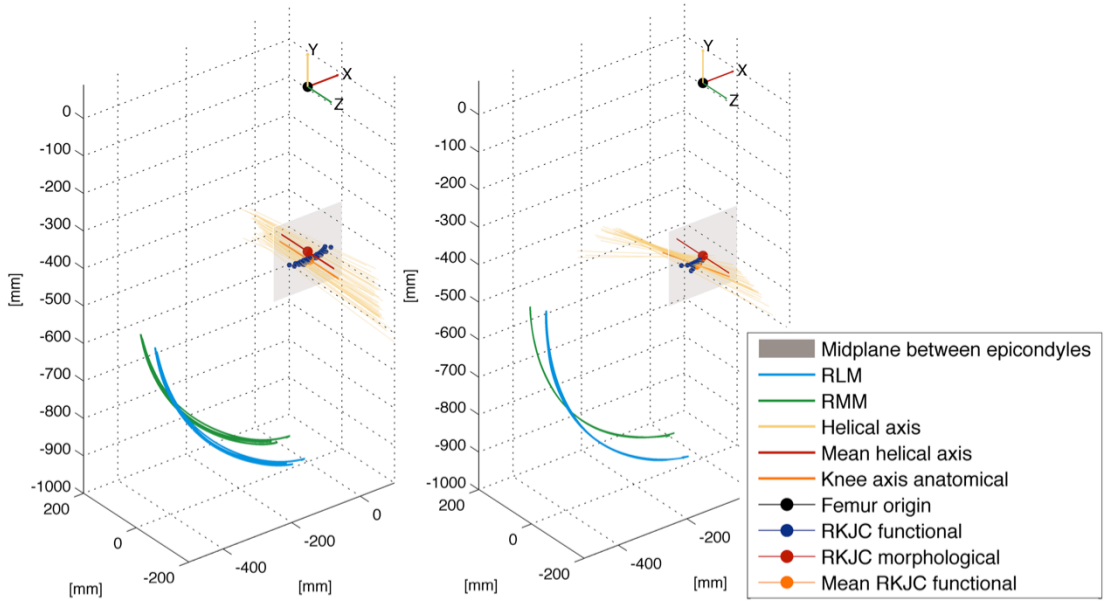

Figure 17. *IHA of loaded and unloaded knee*
Left: loaded knee. Behaves like a sliding knee joint. Right: unloaded knee. Behaves more like a pure hinge joint.

It can be seen that the loaded knee situations shows more translation than the unloaded situation. In this person the direction of loaded knee axis is closer to the regression based morphological knee axis than the unloaded one. This is rather coincidentally and does not hold for all subjects. Figure 18 and 19 show the direction vector and a point on the IHA plotted over time and against flexion angle. It can be seen that the loaded knee axis shows a flexion angle dependent translation. This effect is less visible in the unloaded knee situation. However the unloaded knee data is a lot noisier, which makes is more difficult to read. IHA estimations in the other two subjects show even more noise.

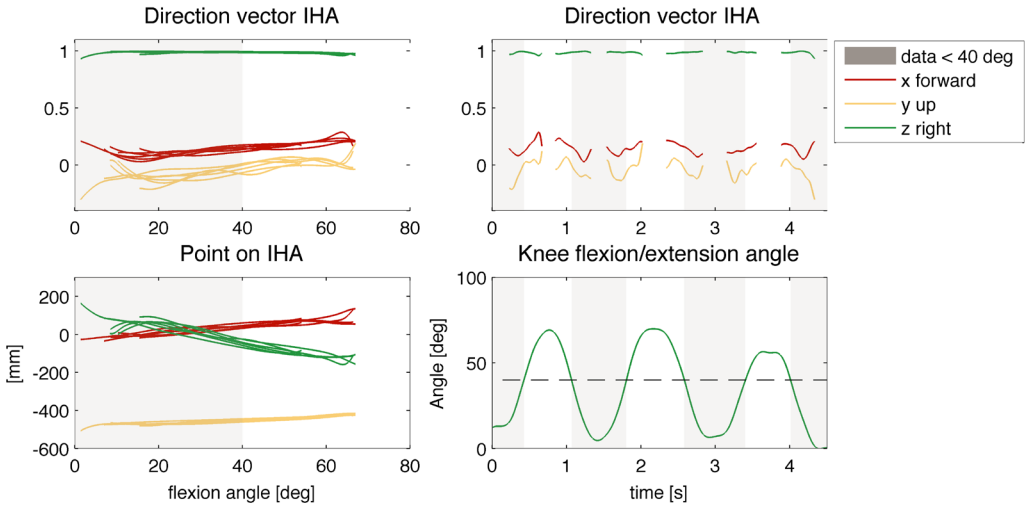

Figure 18. *IHA loaded knee*
IHA of the right knee of subject 1 during loaded knee flexion. Shaded areas represent stance phase with knee flexion angles below 40 degrees. It can be seen that the loaded knee axis shows a flexion angle dependent translation of a point on the IHA (bottom left).

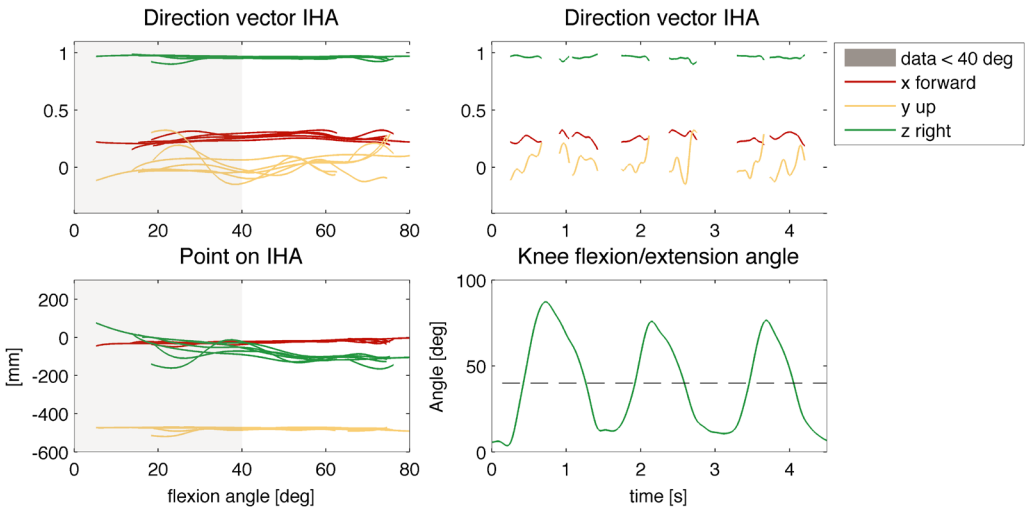

Figure 19. *IHA unloaded knee*
IHA of the right knee of subject 1 during unloaded knee flexion

Appendix C2.3 Knee joint centre and rotation axis estimations

Table 8 shows the marker-based and functional knee joint calibration data for all subjects. Functional knee joint data is given for both the loaded and unloaded knee situation. The loaded knee joint data under 40 degrees of knee flexion is used for the calculation of the mean IHA. The point of the mean IHA intersecting the midplane between the epicondyles was taken to be the centre of the knee joint. This point was used as a scaling point in the functional models.

Table 9. *Loaded and unloaded knee joint calibration*
Marker-based and functional knee joint calibration data of all subjects. The functional knee joint data is given for both loaded and unloaded situation.

Subject 1	**Right knee**			**Left knee**		
	x	*y*	*z*	*x*	*y*	*z*
MB knee centre (mm)	0	-456.83	0	0	-488.30	0
FC knee centre loaded (mm)	-2.09	-464.10	0	11.06	-479.20	0
FC knee centre unloaded (mm)	-2.83			-473.12		
MN knee axis dir.	0	0	0	-16.40	-493.74	0
FC knee axis dir. loaded	0.10	-0.01	1	0	0	1
FC knee axis dir. unloaded	0.26	0.04	0.99	0.02	0.12	0.99
FC knee axis orientation loaded (deg.)	-5.67	-5.94	0.96	-0.10	-0.02	0.99
FC knee axis orientation unloaded (deg.)	4.78	-15.06	-0.30	6.75	-1.07	0.06
Subject 2						
MB knee centre (mm)	0	-419.51	0	0	-434.22	0
FC knee centre loaded (mm)	-55.92	-423.74	0	29.66	-395.69	0
FC knee centre unloaded (mm)	-29.19	-471.54	0	-17.34	-433.02	0
MN knee axis dir.	0	0	1	0	0	1
FC knee axis dir. loaded	0.29	-0.19	0.91	-0.13	0.06	0.97
FC knee axis dir. unloaded	0.44	0.10	0.84	-0.18	-0.14	0.96
FC knee axis orientation loaded (deg.)	-11.49	-17.42	-1.77	3.76	7.43	-0.24
FC knee axis orientation unloaded (deg.)	6.94	-27.27	1.69	-8.34	10.36	0.76
Subject 3						
MB knee centre (mm)	0	-402.74	0	0	-423.58	0
FC knee centre loaded (mm)	-49.72	-388.53	0.0	-53.74	-422.90	0
FC knee centre unloaded (mm)	-20.48	-417.28	0	-29.23	-447.87	0
MN knee axis dir.	0	0	1	0	0	1
FC knee axis dir. loaded	0.20	-0.15	0.96	-0.42	0.16	0.88
FC knee axis dir. unloaded	-8.73	-11.40	-0.87	10.05	25.38	-2.27
FC knee axis orientation loaded (deg.)	0.16	0.02	0.97	-0.35	0.01	0.89
FC knee axis orientation unloaded (deg.)	1.41	-9.30	0.11	0.82	21.68	-0.16

Appendix C2.4 Remarks

Orientation angles of subject 2 and 3 are rather large compared to values found in literature. Griffin, et al. [24] found differences between the transepicondylar axis and the surgical epicondylar axis of 3.7° ± 2.2° on average in patients with osteoarthritic knees. These two axes can be compared with the marker-based and functionally determined knee axis is this research. The large orientation angles of the knee axes found in this study might therefore not be realistic. A possible explanation can be that the marker data was too noisy to accurately estimate the knee axis. By averaging the data over more squatting movements the knee axis will presumably become more accurate.

Appendix D | Kinematics

All gait data presented in this section is averaged over at least 3 gait cycles to reduce abnormalities. Figure 20 shows the joint angles of the left and right leg of an average subject for which subject 2 was chosen. Hip joint angles are given in anatomical directions as well as a total rotation of the femur relative to the pelvis. The bottom plots show the differences in joint angles of the FC and KT models compared to the MB model. Table 9 shows the differences in peak angles for the FC and SK models compared to the MB and KF models respectively. Table 10 shows the mean differences in peak angles averaged over all subjects including both legs.

Appendix D.1 Conclusions and remarks

Appendix D.1.1 Effect of calibration methods

FC methods have large effect on joint angles. Hip ad/abduction and endo/exorotation angles are most affected by functional calibration. However when looking at the total hip rotation angle the effect is less visible. The orientation of the knee axis causes the largest differences in hip endo/exorotation angles. On average hip rotation angles deviate up to 6.19**°**, with a maximum of 14.54**°**. Average knee angle differences were ranging up to 2.60**°** with a maximum of 4.99**°** and the maximum average ankle angle difference was 2.40**°**, with an overall maximum of 3.87**°**.

Appendix D.1.2 Effect of knee translation

Knee translation has a negligible effect on joint angles, with average differences below 1**°.**

Appendix D.1.3 Remarks

Joint angles of the functional models were sometimes strongly deviating from expected joint angles as presented in norm data form literature. This can for example be seen in figure 20 for the hip flexion/extension angles and endo- and exorotation angles. The deviation in hip flexion/extension angles might be a result of scaling. Because the pelvic proportions of the generic model strongly deviate from the proportions in the female subjects an error occurs in marker placement of the markers that are used in inverse kinematics. The deviation in hip endo-exorotation is probably caused by overestimation of the orientation angle of the knee axis as was explained in Appendix C2.2 | Functional knee joint calibration.

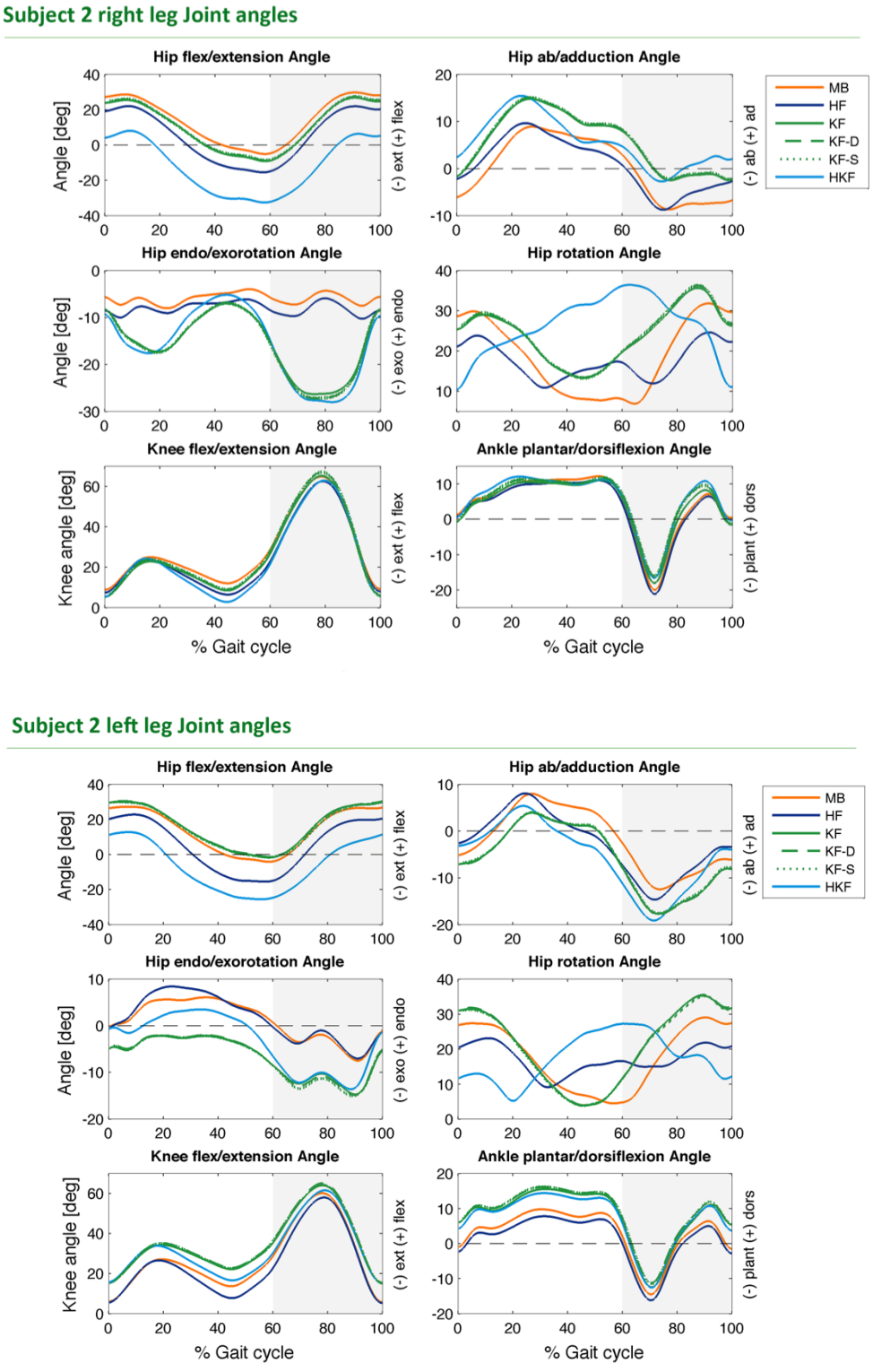

Figure 20. *Joint angles of average subject*
Joint angles of the right and left leg of subject 2 during UI gait estimated with different models: (MB) marker-based, (HF) functional hip, (KF) functional knee, (KF-D) functional knee with knee translation as proposed by Delp, (KF-S) functional knee with knee translation only in stance phase, (HKF) and functional hip and knee.

Table 10. *Joint angle differences*

Differences in peak joint angles are presented in degrees. Differences in peak angles of FC models are compared to MB model and differences of SK models are compared to KF models. Peak angle differences for hip flexion/extension, hip adduction/abduction, hip endorotation/exorotation, total hip rotation, knee flexion/extension and ankle flexion/extension movements are given for both right (R) and left leg (L) of each subject during UI gait.

		Hip flex/ext		**Hip ab/ad**		**Hip endo/exo**		**Hip rot**		**Knee flex/ext**		**Ankle flex/ext**		***Average***
		R	***L***	***R***	***L***	***R***	***L***	***R***	***L***	***R***	***L***	***R***	***L***	
Subject 1														
FC	**HF**	1.46	1.22	2.77	2.17	0.29	0.78	2.31	1.24	0.41	0.49	2.08	0.27	*1.29*
	KF	0.51	1.11	2.31	1.34	6.2	0.34	0.84	1.66	0.46	1.35	0.54	0.91	*1.47*
	HKF	1.86	2.99	1.99	2.36	5.57	1.87	4.28	3.54	1.16	2.11	1.74	0.52	*2.5*
SK	**KF-D**	0.23	0.2	0.08	0.05	0.73	0.36	0.06	0.16	1.33	1.43	0.43	0.86	0.32
	KF-S	0.05	0.23	0.01	0.08	0.57	0.31	0.06	0.25	0.59	0.44	0.11	0.94	0.17
Subject 2														
FC	**HF**	7.7	4.41	0.74	2.21	2.22	0.89	7.16	5.94	2.33	2.15	1.17	1.69	*3.22*
	KF	2.91	2.93	5.89	5.22	18.21	7.22	3.83	6.23	0.39	3.92	1.95	1.04	*4.98*
	HKF	2.75	1.68	6.51	6.63	19.92	6.1	4.6	1.81	1.94	1.42	3.37	0.11	*4.74*
SK	**KF-D**	0.45	0.37	0.23	0.16	0.88	0.1	0.6	0.2	1.78	1.07	1.92	0.61	0.62
	KF-S	0.18	0.11	0.04	0.13	0.6	0.32	0.21	0.07	1.08	0.14	1.65	0.64	0.34
Subject 3														
FC	**HF**	0.41	2.72	0.41	0.19	17.72	21.72	2.34	5.66	1.02	0.92	2.03	2.34	*4.79*
	KF	3.57	4.72	0.17	0.48	12.03	26.19	0.74	9.66	4.35	3.03	0.35	4.27	*5.8*
	HKF	11.17	4.34	0.31	0.01	19.78	24.73	14.54	8.39	3.09	0.65	1.26	7.39	*7.97*
SK	**KF-D**	0.13	0.04	0	0.13	0.5	0.72	0.13	0.48	1.65	1.85	1.42	0.07	0.04
	KF-S	0.24	0.13	0.05	0.22	0.49	0.61	0.02	0.22	1.32	1.14	1.68	0.04	0.03

Table 11. *Average differences joint angles*

Mean differences in peak joint angles in degrees for hip knee and ankle. Differences in peak joint angles presented in degrees. Differences in peak angles of FC models are compared to MB model and differences of SK models are compared to KF models. Hip flexion/extension, ab/adduction and exo/endorotation angles are presented as total hip rotation angle. Absolute values are averaged over three subjects including both legs of each subject during UI gait.

		Hip rot	***SD***	**Knee flex/ext**	***SD***	**Ankle flex/ext**	***SD***	***Average***
FC	**HF**	4.11	*± 2.44*	1.22	*± 0.83*	1.60	*± 0.76*	*2.31*
	KF	3.83	*± 3.55*	2.25	*± 1.75*	1.51	*± 1.46*	*2.53*
	HKF	6.19	*± 4.62*	1.73	*± 0.85*	2.40	*± 2.70*	*3.44*
SK	**KF-D**	0.24	*± 0.15*	0.11	*± 0.08*	0.55	*± 0.29*	*0.15*
	KF-S	0.16	*± 0.07*	0.09	*± 0.08*	0.48	*± 0.14*	*0.12*

Appendix E Kinetics

Appendix E1 Joint moments

All gait data presented in this section is averaged over at least 3 gait cycles to reduce abnormalities. Figure 21 shows the joint moments of the left and right leg of an average subject. Table 11 shows the differences in peak moments of the FC and SK models presented as a percentage of the peak moment of the MB and KF model respectively. Table 12 shows the mean differences in peak moments averaged over all subjects including both legs.

Appendix E2 Conclusions and remarks

Appendix E2.1 Effect of calibration methods

Hip endo/exorotation moments and knee flexion/extension moments are most affected by functional calibration, with maximum mean differences of 25.08 and 24.81%. Because the HF model shows only small deviations it can be concluded that these differences are mainly caused by the rotation of the knee axis.

Appendix E2.2 Effect of knee translation

Knee translation has a small effect on joint moments. Only the mean knee joint moment is affected with a mean maximum of 5.44%.

Appendix E2.3 Remarks

Joint moments are comparable to those found in literature.

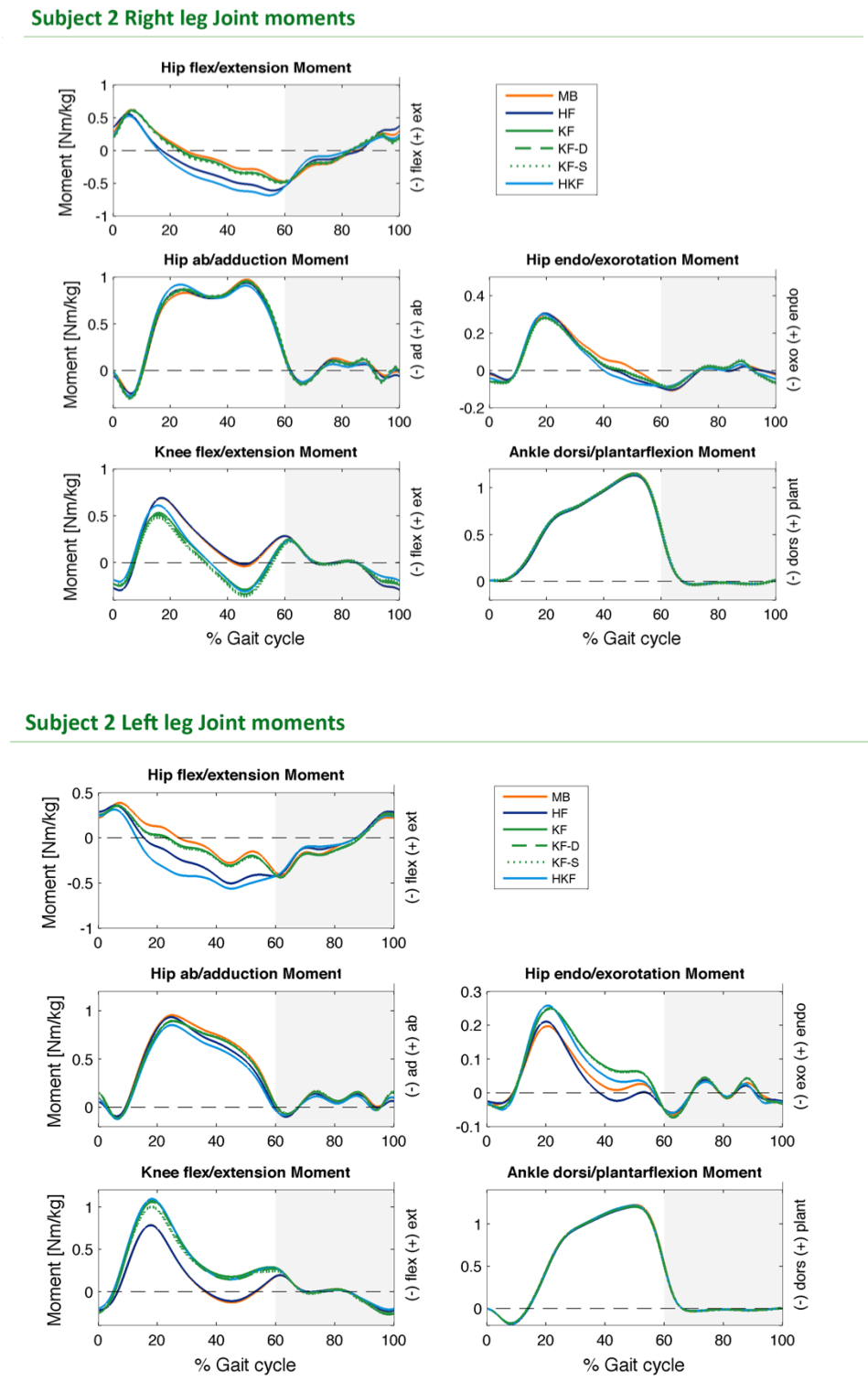

Figure 21. *Joint moments of average subject*

Joint moments of the right and left leg of subject 2 during UI gait estimated with different models: (MB) marker-based, (HF) functional hip, (KF) functional knee, (KF-D) functional knee with knee translation as proposed by Delp, (KF-S) functional knee with knee translation only in stance phase, (HKF) and functional hip and knee.

Table 12. *Joint moment differences*
Differences in peak joint moments of FC models compared to MB models in % of peak MB moments and SK models compared to KF models in % of peak KF joint moments. Peak moments for hip flexion/extension, hip adduction/abduction, hip endorotation/exorotation, knee flexion/extension and ankle flexion/extension movements are given for both right (R) and left leg (L). The average value is given to compare the overall influence of the different models on joint kinetics.

		Hip flex/ext		**Hip ab/ad**		**Hip endo/exo**		**Knee flex/ext**		**Ankle flex/ext**		***Average***
		R	*L*	*R*	*L*	*R*	*L*	*R*	*L*	*R*	*L*	
Subject 1												
FC	**HF**	7.18	5.14	0.32	5.99	3.49	1.66	5.60	1.44	1.61	0.21	*3.26*
	KF	1.80	0.81	0.46	1.73	1.83	5.79	4.59	5.30	0.04	1.12	*2.35*
	HKF	10.00	4.24	2.04	4.73	0.95	3.83	7.44	7.41	1.02	2.60	*4.43*
SK	**KF-D**	0.07	1.34	0.15	0.05	0.25	0.15	1.11	1.15	0.10	0.17	*0.45*
	KF-S	0.56	3.10	0.09	0.12	0.02	0.43	4.65	1.48	0.17	0.24	*1.09*
Subject 2												
FC	**HF**	0.71	22.48	3.58	2.04	1.92	6.79	0.60	0.11	2.05	1.59	*4.19*
	KF	1.12	5.75	1.94	6.25	6.20	27.22	22.90	36.77	0.87	1.55	*11.06*
	HKF	11.28	36.58	5.61	10.74	0.42	30.87	11.21	39.45	0.68	0.44	*14.73*
SK	**KF-D**	0.56	0.81	0.21	0.27	0.19	1.15	3.14	1.98	0.18	0.12	*0.86*
	KF-S	0.20	0.48	0.31	0.12	0.01	0.57	6.29	9.31	0.14	0.13	*1.76*
Subject 3												
FC	**HF**	6.66	6.83	8.70	4.11	22.88	12.36	3.10	1.31	1.07	2.86	*6.99*
	KF	1.85	0.89	5.32	3.18	52.56	41.83	49.07	22.38	3.66	0.68	*18.14*
	HKF	3.77	6.20	5.54	8.13	83.28	31.10	71.90	11.47	9.45	3.70	*23.45*
SK	**KF-D**	0.78	0.30	0.21	0.35	0.47	0.09	10.32	0.82	0.26	0.10	*1.37*
	KF-S	2.16	0.36	0.45	0.63	0.72	0.29	9.64	1.29	0.10	0.07	*1.57*

Table 13. *Mean differences in joint moments*
Average differences in peak moments of FC models in % of peak moments of MB model and SK models in % of peak moments of KF model. Values are averaged over three subjects including both legs of each subject.

		Hip flex/ext		**Hip ab/ad**		**Hip endo/exo**		**Knee flex/ext**		**Ankle flex/ext**		***Average***
		%	*SD*	%	*SD*	%	*SD*	%	*SD*	%	*SD*	
FC	**HF**	8.17	*± 7.41*	4.12	*± 2.95*	8.18	*± 8.24*	2.03	*± 2.02*	1.57	*± 0.89*	4.81
	KF	2.04	*± 1.87*	3.15	*± 2.24*	22.57	*± 21.32*	23.50	*± 17.44*	1.32	*± 1.25*	10.52
	HKF	12.01	*± 12.41*	6.13	*± 2.99*	25.08	*± 31.93*	24.81	*± 26.07*	2.98	*± 3.41*	14.20
SK	**KF-D**	0.64	*± 0.44*	0.21	*± 0.10*	0.38	*± 0.40*	3.09	*± 3.64*	0.16	*± 0.06*	0.90
	KF-S	1.14	*± 1.20*	0.29	*± 0.22*	0.34	*± 0.29*	5.44	*± 3.66*	0.14	*± 0.06*	1.47

Appendix E3 Joint power

All gait data presented in this section is averaged over at least 3 gait cycles to reduce abnormalities. Figure 22 shows the joint power of the left and right leg of an average subject. The bottom plots show the differences in joint power of the functional-based models compared to the marker-based model. The largest differences are displayed in the top of the graphs. Table 14 shows the differences in peak power of the FC and SK models presented as a percentage of the peak power of the MB and KF model respectively. Table 15 shows the mean differences in peak power averaged over all subjects including both legs.

Appendix E4 Conclusions and remarks

Appendix E4.1 Effect of calibration methods

Joint calibration strongly affects hip and knee powers. Hip powers are mostly affected by hip calibration with a maximum mean difference of 36.34% and knee powers mostly by the combined hip and knee calibration with a 37.60% difference.

Appendix E4.2 Effect of knee translation

Knee translation has limited effect on joint powers. A maximum mean difference of 4.87% in hip power was found.

Appendix E4.3 Remarks

Joint moments are comparable to those found in literature.

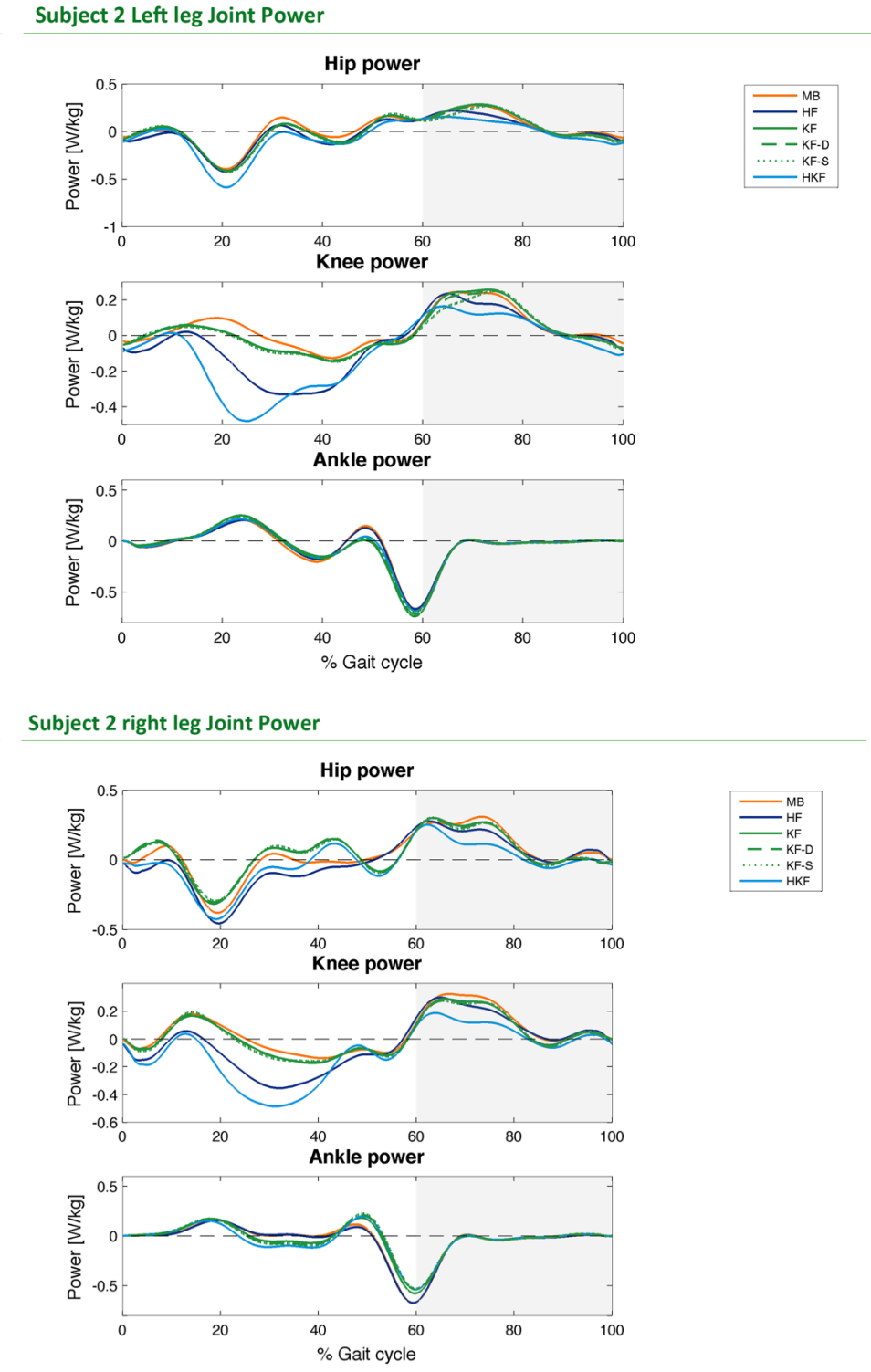

Figure 22. *Joint power of average subject*
Joint power of the right and left leg of subject 2 during UI gait estimated with different models: (MB) marker-based, (HF) functional hip, (KF) functional knee, (KF-D) functional knee with knee translation as proposed by Delp, (KF-S) functional knee with knee translation only in stance phase, (HKF) and functional hip and knee.

Table 14. *Joint power differences*

Differences in peak joint power of FC models compared to MB models in % of peak MB moments and SK models compared to KF models in % of peak KF joint moments. Peak power for hip flexion/extension, hip adduction/abduction, hip endorotation/exorotation, knee flexion/extension and ankle flexion/extension movements are given for both right (R) and left leg (L). The average value is given to compare the overall influence of the different models on joint kinetics.

		Hip		**Knee**		**Ankle**		***Average***
		R	*L*	*R*	*L*	*R*	*L*	
	Subject 1							
FC	**HF**	73.56	7.01	10.00	5.03	7.87	0.21	*17.28*
	KF	4.20	1.28	22.63	4.52	3.28	5.20	*6.85*
	HKF	36.90	12.01	26.57	6.89	5.38	7.50	*15.87*
SK	**KF-D**	2.16	2.87	0.82	4.13	2.98	5.00	*2.99*
	KF-S	5.39	7.05	1.18	0.80	4.41	3.36	*3.70*
	Subject 2							
FC	**HF**	19.78	13.54	9.45	35.88	0.31	0.24	*13.20*
	KF	17.15	1.16	11.05	5.86	13.99	10.64	*9.97*
	HKF	11.71	59.85	49.91	97.51	19.90	3.01	*40.32*
SK	**KF-D**	3.00	0.07	4.04	3.07	5.70	3.56	*3.24*
	KF-S	3.99	3.07	3.55	2.55	6.94	6.29	*4.40*
	Subject 3							
FC	**HF**	73.56	30.00	10.00	20.57	7.87	4.48	*24.41*
	KF	4.20	40.58	22.63	1.02	3.28	2.93	*12.44*
	HKF	36.90	13.75	26.57	18.15	5.38	0.96	*16.95*
SK	**KF-D**	2.16	1.52	0.82	2.44	2.98	2.12	2.01
	KF-S	5.39	4.32	1.18	4.00	4.41	2.87	3.70

Table 15. *Mean power differences*

Average differences in peak power of FC models in % of peak power of MB model and SK models in % of peak power of KF model. Values are averaged over three subjects including both legs of each subject.

		Hip		**Knee**		**Ankle**		***Average***
		%	*SD*	*%*	*SD*	*%*	*SD*	%
FC	**HF**	36.24	± 29.88	15.16	± 11.38	3.50	± 3.76	18.30
	KF	11.43	± 15.46	11.29	± 9.36	6.55	± 4.66	9.76
	HKF	28.52	± 19.47	37.60	± 32.57	7.02	± 6.70	24.38
SK	**KF-D**	1.96	± 1.07	2.55	± 1.48	3.72	± 1.36	2.75
	KF-S	4.87	± 1.39	2.21	± 1.36	4.71	± 1.60	3.93

8.2 Appendix F | Muscle-tendon outcome

All gait data presented in this section is averaged over at least 3 gait cycles to reduce abnormalities. The effect functional calibration and knee translation on muscle-tendon (MT) length and velocity is shown.

Appendix F1 | Muscle-tendon length

Figure 23 shows the MT length of the psoas, semimembranosus and gastrocnemius muscle of the left and right leg of an average subject. Absolute MT lengths are given (top plots) and MT lengths normalized with MT rest-length (bottom plots). Normalized lengths and velocities are used in clinic to determine whether a muscle is too short or too slow. The absolute length of the muscle is in that case less important because, the shape of the MT length and velocity curves determine whether a muscle is to be classified as too short or too slow.
Table 16 shows the differences in peak MT length of the FC models compared to the MB model and the KT models compared to the KF model for each subject during UI and CP gait. Differences are presented as a percentage of peak MT length of the MB and KF model respectively. Table 17 shows the average differences over all subjects.

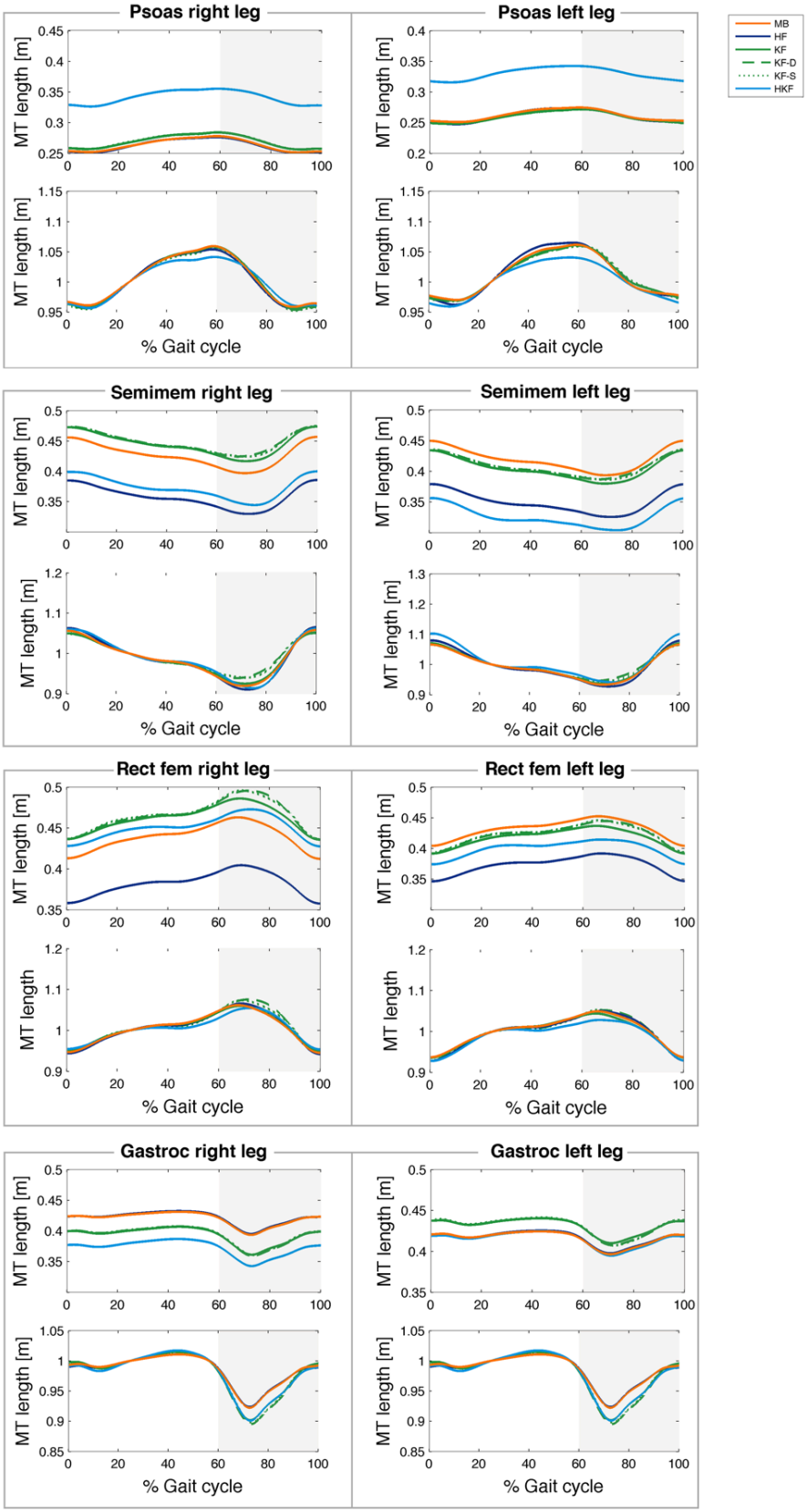

Figure 23. *MT lengths of average subject absolute and normalized*
MT lengths of left and right leg subject 2. For each muscle MT lengths are plotted at absolute length (top plots) and normalized with MT rest length (bottom plots).

***Table 16**. MT length differences*
Differences in MT length of FC models compared to MB models in % of peak MT lengths of the MB model and SK models compared to KF models. Absolute MT length differences of psoas, semimembranosus and gastrocnemius muscle are given for both legs (L and R) of all subjects during unimpaired (UI) gait and Cerabral Palsy (CP) mimicking gait.

			Psoas		**Semimem.**		**Rectus fem.**		**Gastroc.**		***Average***
			R	*L*	*R*	*L*	*R*	*L*	*R*	*L*	
Subject 1											
UI	**FC**	**HF**	2.84	2.15	6.40	3.52	7.35	3.92	0.19	0.03	3.30
		KF	0.55	0.82	1.93	1.94	2.22	2.06	2.65	2.60	1.85
		HKF	0.29	0.01	2.28	1.82	3.84	2.96	3.90	0.20	1.91
	SK	**KF-D**	0.01	0.01	0.15	0.29	2.74	2.55	0.13	0.15	0.75
		KF-S	0.01	0.01	0.14	0.36	2.07	2.00	0.18	0.33	0.64
CP	**FC**	**HF**	1.76	1.02	3.53	0.49	3.54	0.11	0.69	0.32	*1.43*
		KF	2.01	0.49	5.49	1.07	6.23	1.86	3.90	1.93	*2.87*
		HKF	1.61	1.22	1.25	1.28	0.05	0.94	5.00	0.85	*1.53*
	SK	**KF-D**	0.19	0.15	1.32	1.59	3.36	3.34	0.45	0.60	*1.38*
		KF-S	0.20	0.21	1.65	1.65	2.12	2.01	0.10	0.64	*1.07*
Subject 2											
UI	**FC**	**HF**	0.60	0.30	15.53	15.67	12.62	13.37	0.25	0.22	7.32
		KF	2.20	1.06	3.71	3.44	4.96	3.46	5.64	3.75	3.53
		HKF	27.64	24.56	12.42	20.73	2.11	8.38	10.25	0.06	13.27
	SK	**KF-D**	0.09	0.07	0.22	0.36	2.06	1.76	0.09	0.07	0.59
		KF-S	0.01	0.07	0.10	0.33	2.12	2.02	0.11	0.23	0.62
CP	**FC**	**HF**	0.22	0.65	15.66	16.20	12.31	13.09	0.37	0.23	*7.34*
		KF	2.69	0.76	4.42	3.63	5.22	3.72	7.05	3.37	*3.86*
		HKF	30.45	26.45	12.10	21.82	3.19	7.47	11.62	0.32	*14.18*
	SK	**KF-D**	0.03	0.08	1.08	1.35	2.64	2.73	0.06	0.37	*1.04*
		KF-S	0.11	0.35	1.35	1.54	2.19	2.03	0.40	0.15	*1.02*
Subject 2											
UI	**FC**	**HF**	4.41	3.89	16.72	17.07	12.99	14.16	0.15	0.18	8.70
		KF	0.52	1.41	1.47	0.67	2.22	0.07	5.18	1.84	1.67
		HKF	18.69	20.82	11.30	3.17	2.57	6.50	6.81	17.40	10.91
	SK	**KF-D**	0.06	0.07	0.08	0.10	1.54	1.89	0.04	0.05	0.48
		KF-S	0.12	0.12	0.21	0.23	1.91	2.05	0.01	0.03	0.59
CP	**FC**	**HF**	4.48	3.64	18.12	18.54	12.63	13.42	0.24	0.12	*8.90*
		KF	0.92	1.89	1.13	2.13	1.61	0.34	3.84	0.37	*1.53*
		HKF	20.39	22.33	12.31	2.47	1.71	6.62	7.54	20.26	*11.70*
	SK	KF-D	0.02	0.02	0.96	1.14	2.73	2.89	0.31	0.19	*1.03*
		KF-S	0.03	0.06	1.27	1.37	1.82	1.90	0.07	0.04	*0.82*

Table 17. *Average MT length differences*
Average of absolute MT peak length differences over all subjects psoas, semimembranosus and gastrocnemius muscle, presented as % of peak length of marker-based model and as absolute value in mm.

			Psoas		**Semimem.**		**Rectus fem.**		**Gastroc.**		***Average***
			%	*SD*	*%*	*SD*	*%*	*SD*	*%*	*SD*	***%***
UI	**FC**	**HF**	2.37	*± 1.68*	12.49	*± 5.93*	10.74	*± 4.13*	0.17	*± 0.08*	6.44
		KF	1.09	*± 0.64*	2.19	*± 1.17*	2.50	*± 1.63*	3.61	*± 1.53*	2.35
		HKF	15.34	*± 12.16*	8.62	*± 7.54*	4.39	*± 2.50*	6.44	*± 6.65*	8.70
	SK	**KF-D**	0.05	*± 0.03*	0.20	*± 0.11*	2.09	*± 0.47*	0.09	*± 0.04*	0.61
		KF-S	0.06	*± 0.05*	0.23	*± 0.10*	2.03	*± 0.07*	0.15	*± 0.12*	0.62
CP	**FC**	**HF**	1.96	*± 1.72*	12.09	*± 7.94*	9.18	*± 5.81*	0.33	*± 0.20*	5.89
		KF	1.46	*± 0.86*	2.98	*± 1.82*	3.16	*± 2.28*	3.41	*± 2.24*	2.75
		HKF	17.08	*± 12.62*	8.54	*± 8.32*	3.33	*± 3.07*	7.60	*± 7.51*	9.14
	SK	**KF-D**	0.08	*± 0.07*	1.24	*± 0.23*	2.95	*± 0.32*	0.33	*± 0.19*	1.15
		KF-S	0.16	*± 0.12*	1.47	*± 0.16*	2.01	*± 0.14*	0.23	*± 0.24*	0.97

8.2.1 Appendix F2 | Muscle-tendon velocity

Figure 24 shows the MT velocities of the psoas, semimembranosus and gastrocnemius muscle of the left and right leg of an average subject. Absolute MT lengths are given (top plots) and MT lengths normalized with MT rest-length (bottom plots). Normalized lengths and velocities are used in clinic to determine whether a muscle is too short or too slow. The absolute length of the muscle is in that case less important because, the shape of the MT length and velocity curves determine whether a muscle is to be classified as too short or too slow.

Table 18 shows the differences in peak MT velocity of the FC models compared to the MB model and the KT models compared to the KF model for each subject during UI and CP gait. Differences are presented as a percentage of the range of MT velocity of the MB and KF model respectively. Table 19 shows the average differences over all subjects.

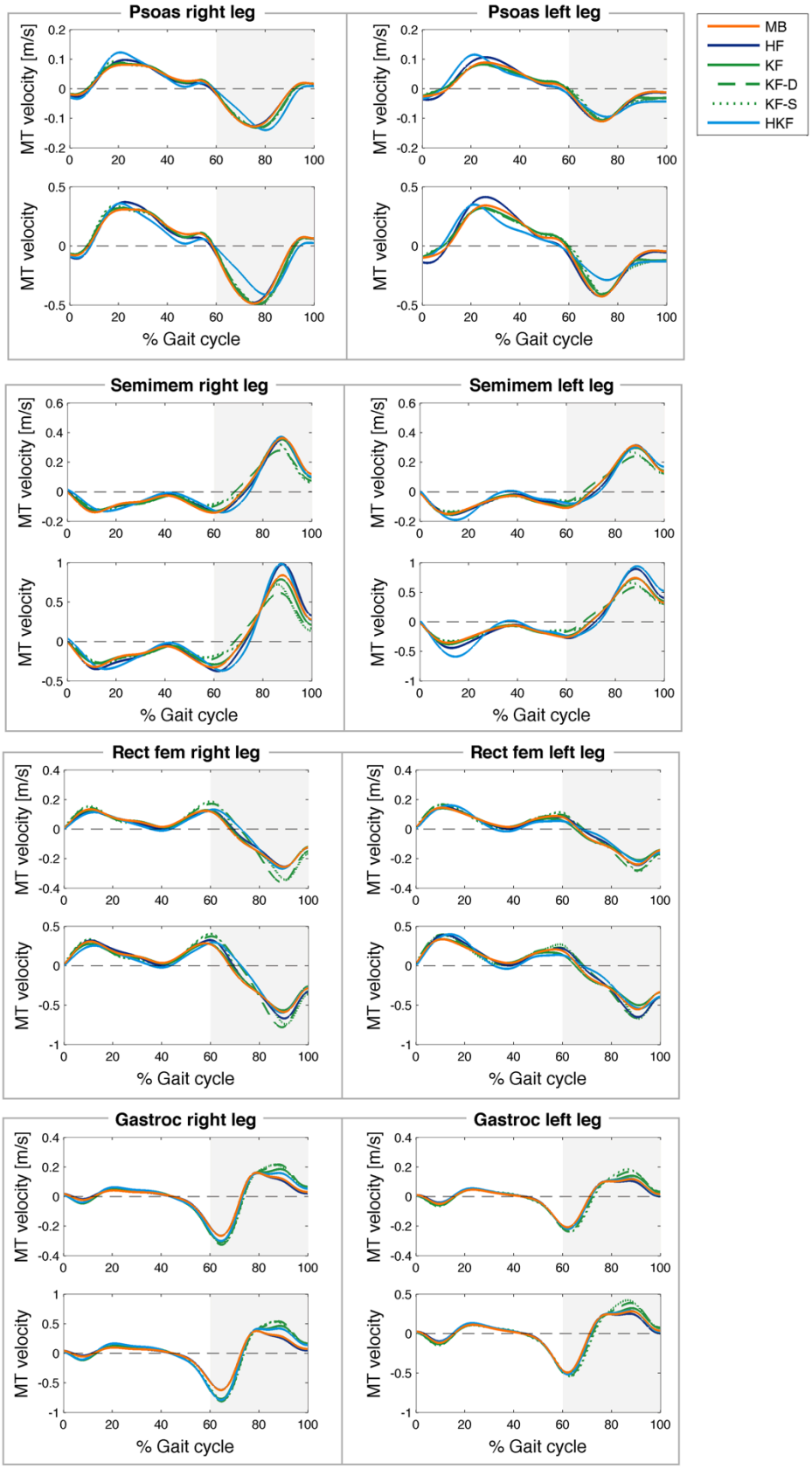

Figure 24. *MT velocities of average subject absolute and normalized MT velocity of left and right leg of subject 2. For each muscle MT velocity are plotted at absolute velocity (top plots) and normalized (bottom plots).*

Table 18. *MT Velocity differences*

Peak differences in % of peak MT velocity of MB model. Absolute MT velocity differences of psoas, semimembranosus and gastrocnemius muscle are given for both legs (L and R) of all subjects during unimpaired gait.

			Psoas		**Semimem.**		**Rectus fem.**		**Gastroc.**		***Average***
			R	*L*	*R*	*L*	*R*	*L*	*R*	*L*	
Subject 1											
UI	**FC**	**HF**	4.98	5.46	0.56	1.07	0.04	0.02	2.71	1.23	2.01
		KF	0.36	0.24	0.85	3.65	0.26	1.24	8.46	3.98	2.38
		HKF	6.31	9.67	0.87	3.89	1.61	0.03	5.12	2.96	3.81
	SK	**KF-D**	1.11	0.40	15.82	21.96	19.09	12.38	12.09	10.12	11.62
		KF-S	1.20	0.07	4.74	5.26	18.90	13.19	12.00	16.20	8.95
CP	**FC**	**HF**	1.17	0.26	0.92	0.37	1.77	0.86	1.40	0.25	0.88
		KF	2.50	1.39	1.20	2.06	2.44	0.99	0.24	2.10	1.62
		HKF	0.84	3.28	0.53	2.08	1.09	0.98	0.65	1.61	1.38
	SK	**KF-D**	0.67	0.81	14.72	21.29	9.38	2.60	13.36	10.25	9.14
		KF-S	0.14	0.85	0.22	1.65	0.95	0.80	15.76	12.86	4.15
Subject 2											
UI	**FC**	**HF**	6.59	7.34	1.34	0.24	2.93	0.26	0.12	2.43	2.66
		KF	1.93	2.64	1.26	3.24	1.46	0.81	6.40	4.19	2.74
		HKF	16.99	10.92	1.35	2.00	0.46	2.94	0.43	0.62	4.46
	SK	**KF-D**	1.22	0.20	12.64	12.16	11.75	4.77	7.84	5.57	7.02
		KF-S	2.59	0.02	4.63	5.95	15.90	5.05	7.84	8.56	6.32
CP	**FC**	**HF**	3.59	0.15	0.03	0.73	0.96	0.05	0.48	0.14	0.77
		KF	2.44	1.32	0.15	4.33	0.94	0.86	3.95	1.04	1.88
		HKF	5.80	0.01	3.30	2.89	2.03	3.92	0.92	0.53	2.43
	SK	**KF-D**	0.55	0.40	9.18	10.34	3.65	2.78	5.86	2.66	4.43
		KF-S	1.04	0.80	0.22	0.48	1.09	0.34	8.88	5.09	2.24
Subject 3											
UI	**FC**	**HF**	10.12	4.95	0.14	11.00	0.06	1.94	0.93	6.62	4.47
		KF	1.81	5.81	1.08	6.66	0.36	2.13	0.06	15.15	4.13
		HKF	14.72	0.47	1.00	1.53	5.41	4.56	2.17	10.60	5.06
	SK	**KF-D**	0.58	0.37	14.56	23.96	6.22	11.16	1.63	5.40	7.99
		KF-S	0.89	0.65	8.67	11.80	11.22	13.56	2.56	8.77	7.27
CP	**FC**	**HF**	6.63	2.27	0.92	1.80	5.28	0.15	1.75	1.26	2.51
		KF	0.15	1.76	4.77	5.06	2.79	1.08	1.01	1.93	2.32
		HKF	1.78	4.24	3.67	1.90	9.62	1.63	0.61	0.31	2.97
	SK	**KF-D**	0.71	0.46	16.45	26.02	13.28	9.70	6.96	6.64	10.03
		KF-S	2.68	0.41	1.76	0.08	7.30	1.21	9.29	12.57	4.41

Table 19. *Average MT velocity differences*
Average of absolute MT peak velocity differences over all subjects psoas, semimembranosus and gastrocnemius muscle, presented as % of peak velocity of marker-based model and as absolute value in mm/s.

			Psoas		**Semimem.**		**Rectus fem.**		**Gastroc.**		***Average***
			%	*SD*	*%*	*SD*	*%*	*SD*	*%*	*SD*	***%***
UI	**FC**	**HF**	6.57	*± 1.98*	2.39	*± 4.24*	0.88	*± 1.25*	2.34	*± 2.31*	3.05
		KF	2.13	*± 2.03*	2.79	*± 2.23*	1.04	*± 0.71*	6.37	*± 5.13*	3.08
		HKF	9.85	*± 5.94*	1.77	*± 1.11*	2.50	*± 2.19*	3.65	*± 3.81*	4.44
	SK	**KF-D**	0.65	*± 0.42*	16.85	*± 4.95*	10.90	*± 5.09*	7.11	*± 3.73*	8.88
		KF-S	0.90	*± 0.95*	6.84	*± 2.85*	12.97	*± 4.69*	9.32	*± 4.54*	7.51
CP	**FC**	**HF**	2.35	*± 2.47*	0.80	*± 0.60*	1.51	*± 1.95*	0.88	*± 0.67*	1.38
		KF	1.59	*± 0.87*	2.93	*± 2.07*	1.52	*± 0.86*	1.71	*± 1.29*	1.94
		HKF	2.66	*± 2.18*	2.40	*± 1.14*	3.21	*± 3.32*	0.77	*± 0.46*	2.26
	SK	**KF-D**	0.60	*± 0.16*	16.33	*± 6.45*	6.90	*± 4.49*	7.62	*± 3.71*	7.86
		KF-S	0.99	*± 0.89*	0.74	*± 0.76*	1.95	*± 2.64*	10.74	*± 3.76*	3.60